

Figure 18.11 Solid lines show north-south length scales (wavelength/ 2π) and dashed lines shown trapping scales (e-folding distance) for barotropic waves generated by a meandering current with inverse frequency ω^{-1} and inverse wavenumber k^{-1} . Eastward going meanders ($k > 0$) produce trapped waves; westward going meanders ($k < 0$) may produce propagating disturbances. The symbols \otimes correspond to typical observational estimates of ω^{-1} and k^{-1} .

oceanographers; however, we include it to illustrate some of the effects of the z structure. If we substitute $\Psi(y, z) = S^{1/4}\Phi(y, \zeta)$, where $\zeta = \int_{z-H}^z S^{1/2}(z') dz'$ is a modified vertical coordinate, we find

$$\left(\frac{\partial^2}{\partial y^2} + \frac{\partial^2}{\partial \zeta^2}\right) \Phi + \nu^2(y, \zeta)\Phi = 0,$$

where the index of refraction $\nu^2(y, \zeta)$ is given by

$$\nu^2(y, \zeta) = S^{-1/4} [S^{-1} [S^{1/4}]_z]_z + \frac{\beta - \bar{u}_{yy} - (\bar{u}_z/S)_z}{\bar{u} - \omega/k} - k^2. \quad (18.47)$$

When $\nu^2 > 0$ there are sinusoidal solutions and energy propagates freely, whereas when $\nu^2 < 0$ there are only exponential solutions (along the ray) and the waves die out. There are also, of course, diffraction effects and tunneling effects if the regions of negative ν^2 (or, at least, significantly altered ν^2) are relatively small. This form is useful when N is a simple function (e.g., $N_0 e^{z/d}$) so that the first term in (18.47) is also simple $[-3/(4d^2S)]$. The stratification then contributes a relatively large and negative term which increases toward the bottom, inhibiting penetration into the deep water. For our $S(z)$ profile (figure 18.7), however, numerical differentiation proved to be excessively noisy. Moreover, in the oceans, most of the motions of interest have vertical scales that are significantly influenced by the boundaries and are larger than the scales of variation of ν^2 , so that a local (WKB) interpretation of ν^2 variations is not possible.

We can, however, associate modifications in ν^2 occurring on large scales with modifications in the structure of Ψ . Thus in the topographic problem, if the shear in the vertical is such that

$$\frac{\partial}{\partial z} \frac{1}{S} \frac{\partial \bar{u}}{\partial z} > 0 \quad \text{and} \quad \frac{\partial \bar{u}}{\partial z} > 0,$$

there will be a decrease in the value of ν^2 , implying that the wave will become either more barotropic ($\nu^2 > 0$) or more bottom trapped ($\nu^2 < 0$). In the example of Rossby wave radiation from a meandering Gulf Stream, (18.46) implies that the baroclinic modes ($\lambda_n^2 > 0$) become trapped even more closely than the barotropic modes.

As a final example, we note that the motions forced in the ocean by atmospheric disturbances tend to have large positive ω/k and large scales. In the absence of mean currents, the vertical structure equation, with $\Psi = e^{i\omega t} F(z)$, becomes

$$\frac{\partial}{\partial z} \frac{1}{S} \frac{\partial}{\partial z} F = \left[\frac{\beta k}{\omega} - k^2 - l^2 \right] F = -\nu^2 F, \quad (18.48)$$

implying that the forced currents are nearly barotropic. However, the recent work of Frankignoul and Müller (1979) suggests a possible mechanism by which significant baroclinic currents may be produced. Because the ocean is weakly damped and has resonant modes ($\nu^2 = \lambda_n^2$), even very small forcing near these resonances can cause the energy to build up in these modes. This is another example of the strong influence of the boundaries on the oceanic system.

18.6 Friction in Quasi-Geostrophic Systems

18.6.1 Ekman Layers

Ekman (1902, 1905), acting on a suggestion of Nansen, was the first to explore the influence of the Coriolis force on the dynamics of frictional behavior in the upper wind-stirred layers of the oceans. He considered both steady and impulsively applied, but horizontally uniform, winds. In an effort to understand how surface frictional stresses τ influence the upper motion of the atmosphere and, in particular, how a cyclone "spins down," Charney and Eliassen (1949) were led to consider horizontally varying winds. They showed that Ekman dynamics generates a horizontal convergence of mass in the atmospheric boundary layer proportional to the vertical component of the vorticity of the geostrophic wind in this layer. Thus a cyclone produces a vertical flow out of the boundary layer which compresses the earth's vertical vortex tubes and generates *anticyclonic* vorticity. The time constant for frictional decay in a barotropic fluid was found to be $(f_0 E^{1/2})^{-1}$, where E is the Ekman number $\nu_e / f_0 H^2$, with ν_e the eddy coefficient of viscosity and H the depth of the fluid. Greenspan and Howard (1963) investigated the time-

dependent motion of a convergent Ekman layer: if the wind is turned on impulsively, the Ekman layer is set up in a time of order f_0^{-1} ; the internal flow decays in a time of order $(f_0 E^{1/2})^{-1}$; and the vertical oscillations that are produced by the impulsive startup decay in a time of order $(f_0 E)^{-1}$. Since f_0^{-1} is but a few hours, one may consider that for the large-scale wind and current systems of the atmosphere and oceans the Ekman pumping is produced instantly and that there is a balance in the Ekman layer among the frictional pressure and Coriolis forces. We divide the flow into a quasigeostrophic interior component (u_g, v_g, w_g) with associated pressure gradients $f v_g = \alpha p_{gx}$ etc. and a deviation component associated with the friction (u_e, v_e, w_e) which vanishes below some small depth h . For a homogeneous fluid $p_e = 0$ because the hydrostatic assumption ensures that there can be no nontrivial pressure field which vanishes below $z = -h$. For a stratified flow a scaling argument can be made to show that buoyancy fluctuations in the upper layer will not be important enough to cause significant p_e 's (unless $N^2 > \tau_0 L / \rho h^3$) so that $\rho f v_e = -(\partial/\partial z)\tau \cdot \hat{x}$, etc. If we divide by f , and compute w_e from the divergence of the Ekman horizontal velocities, we find

$$w_e = -\hat{z} \cdot \text{curl}(\tau/\rho f)$$

using $\tau(-h) = 0$, $w_e(-h) = 0$. From the surface condition $w_e(0) + w_g(0) = 0$, the Ekman pumping is therefore

$$w_g(0) \equiv w_E = \hat{z} \cdot \text{curl}(\tau(0)/\rho f), \quad (18.49)$$

where $\tau(0)$ is the wind stress at the sea surface. The same procedure can be used in the lower boundary layer:

$$w_g = \frac{\partial}{\partial x} \left(\frac{v_e v_{ez}}{f} \right) - \frac{\partial}{\partial y} \left(\frac{v_e u_{ez}}{f} \right), \quad z = -H.$$

But now it is necessary to specify $\tau(-H)$ in terms of the geostrophic velocities u_g, v_g ; for this a knowledge of v_e is required. If we assume v_e to be constant, the pumping out of the bottom boundary layer is given by

$$w_g(-H) \equiv w_E = \frac{D_E}{2} \left[\zeta_g + u_{gx} + v_{gy} + \frac{1}{2} (\beta/f)(u_g - v_g) \right] \Big|_{z=-H},$$

where $D_E = (2\nu_e/f)^{1/2}$ and $\zeta_g = v_{gx} - u_{gy}$ is the vorticity of the geostrophic wind. When $L \ll a$, the divergence terms (which are equal to $-\beta v_g/f$) and the last term are negligible, so that

$$w_g(-H) = \frac{D_E}{2} \zeta_g(-H). \quad (18.50)$$

In the lower boundary layer of the deep ocean, the water is nearly homogeneous. In this case one may estimate the bulk viscosity ν_e by supposing that for this value the established boundary layer is marginally

stable (cf. Charney, 1969). From the measurements of Tatro and Mollo-Christensen (1967), the condition for marginal stability is found to be that the Reynolds number based on the depth D_E , of the Ekman layer $UD_E/\nu_e = \sqrt{2}U/\sqrt{f\nu_e}$, shall be of order 100. Thus, for example, $\nu_e \sim U^2/5000f = 200 \text{ cm}^2 \text{ s}^{-1}$, and $D_E \sim U/50f \sim 20 \text{ m}$ for a current of 10 cm s^{-1} in middle latitudes.

In a stratified atmosphere or ocean, the depth of influence of the Ekman pumping is not necessarily the depth of the fluid. If a circulation is forced from above by Ekman pumping with horizontal scale L , one expects the depth of influence to be the vertical deformation radius $H_R \sim f_0 L/N$. This depth will be comparable to the ocean depth for $L \sim L_R = 50 \text{ km}$. Most surface forcing will thus excite a barotropic response. The spin-down of baroclinic mesoscale ocean eddies will be considered in Section 18.6.3.

18.6.2 Spin-Up of the Ocean

The problem of the spin-up of the entire ocean requires definition. The wind and thermally driven circulations are so coupled nonlinearly that it is not possible to treat the establishment of the wind-driven circulation independently. The important question, however, is not how the ocean circulation would be established from rest if the forcing were impulsively applied, but rather how the circulation would change if the forcing changed. The latter question has clear implications for understanding the role of the oceans in climatic change. Thus, one is led to consider first the small-amplitude adjustment of a given steady-state circulation to a change in the wind stress, with the expectation that nonadiabatic changes will require considerably long times. Even for this linearized problem, results for the spin-up of the ocean in mid-latitudes have been obtained (Anderson and Gill, 1975; Anderson and Killworth, 1977; Cane and Sarachik, 1976, 1977) only for the simplest cases of a one- or two-layer model with no preexisting circulation. The solutions for a suddenly applied wind stress are complicated, but their qualitative import can be simply stated. When a steady, east-west wind stress is suddenly applied to a two-layer ocean, initially at rest, the motion at any longitude increases uniformly with time until a non-dispersive Rossby wave starting at the eastern boundary and moving with the maximum westward baroclinic group velocity $-\beta L_R^2$ reaches that longitude. When this occurs, a steady Sverdrup flow induced by the wind-stress curl will have been established in the upper layer everywhere to the east of that longitude. By the time the Rossby wave reaches the western boundary, a steady state will have been established over the entire ocean—except in the vicinity of the boundary itself, where slow-moving reflected Rossby waves influence the flow and are presumed to be dis-

sipated by friction. Thus the spin-up time is essentially the time required for a signal traveling at the speed $-\beta L_R^2$ to cross the ocean from east to west. For width of 6000 km, we obtain 1.5×10^8 or about 5 years.

We note that βL_R^2 increases toward the equator. However, as one approaches the equator the dynamics of wave propagation change. Near the equator, Rossby-gravity and Kelvin waves are generated. These have maximum group velocities of order $\sqrt{g'H}$ (g' is the reduced gravity and H the depth of the thermocline) $\sim 1 \text{ m s}^{-1}$, giving spin-up times of the order of months rather than years. Cane (1979a) and Philander and Pacanowski (1980a) have shown that an impulsively generated uniform westward wind produces both equatorially trapped Kelvin and Rossby-gravity waves. The equatorial undercurrent is established at a given longitude when a Kelvin wave traveling eastward from the western boundary reaches that longitude. The dynamics of equatorially trapped planetary wave modes have been investigated by Rosenthal (1965) and Matsuno (1966) for the atmosphere and by Blandford (1966), Lighthill (1969), and Cane and Sarachik (1979) for the oceans. The dynamics of the equatorial undercurrent has been reviewed by Philander (1973, 1980).

A similar linear analysis for a continuously stratified ocean initially at rest leads to quite different results. In this case, a wind stress can produce a steady Sverdrup transport only in the upper frictional boundary layer. This is the result of the conservation of density, which requires $wS = 0$ or $w = 0$, and it follows from the interior geostrophic dynamics that $\beta v = fw_z = 0$. The initial application of the wind stress will produce an infinity of transient internal baroclinic modes whose sum will approach zero in time everywhere except at $z = 0$. If we consider only the barotropic and first baroclinic modes, the temporal evolution will be similar to that of the two-layer ocean, but the effect of the other modes will be such as to cause all interior velocities to vanish asymptotically in time.

However, if a perturbation in wind stress is applied to *preexisting* flow, Ekman pumping can penetrate into the interior along isopycnals and w_z need not be zero. Although this calculation has not been made in detail, it seems plausible that the final perturbation structure would be similar to the mean-flow structure and, therefore, that it would be spun up in the time associated with the cross-ocean propagation of the lowest baroclinic modes.

It is also important to note that the definition of the spin-up time depends to some degree on the property one is considering. For example, the Sverdrup balance (see Leetmaa, Niiler and Stommel, 1977, for an empirical discussion) is established on relatively short time scales. If the ocean is forced by the Ekman pumping,

$$w_E = w_0 \exp[ikx - i\omega t],$$

it may be seen from the vorticity equation (18.32) that Sverdrup balance will be attained when $|\omega k| \ll \beta$. Thus fluctuations in forcing on the size of the basin with periods even as short as a few days—the time for the *barotropic* wave to cross the basin—will preserve the Sverdrup balance.

Clearly there are many unanswered questions concerning even the adiabatic response of the ocean to changes in the forcing. We know still less about the response time of the entire wind-driven thermohaline circulation, although we expect the time scales to be much longer. The heat and salt transfer processes may take as long as 50 years for transfer down to the main thermocline and 1000 years for formation of the abyssal water beneath the main thermocline.

For the atmosphere, too, the nonadiabatic spin-up or spin-down processes are slower—radiative heat-transfer processes have time constants of the order of months—than the spin-down time of a few days associated with Ekman pumping. Moreover, the calculations in section 18.6.3 indicate that Ekman spin-down will tend only to reduce the barotropic component of the kinetic energy, that is, they reduce the winds by their surface values. Other processes must be involved in the decay of the winds aloft.

18.6.3 Spin-Down of Mesoscale Eddies

As a final example of frictional quasigeostrophic dynamics, we shall consider the effects of bottom friction on mesoscale ocean eddies. In the atmosphere, friction at the ground is an important part of the dynamics of synoptic scale motions. In the ocean, however, friction is considered to be less important because the bottom currents are relatively weak. Nevertheless, it is of interest to know how much of the water column is affected by bottom friction. We do know that the surface manifestations of mesoscale motions (in particular Gulf Stream rings) can persist for longer than 2 years (Cheney and Richardson, 1976). We shall show that this time scale is consistent with predictions of the simple baroclinic spin-down time.

Holton (1965) obtained a solution to the spin-down problem for a uniformly stratified fluid in a cylindrical container, showing that the effects of Ekman pumping are confined to a height $H_R \sim f_0 L/N$. Walin (1969) completed and extended Holton's analysis by analyzing in detail the effects of the side-wall boundaries and gave a simpler illustration of the spin-down process not involving side boundaries. We shall solve the analogue of Walin's problem for the variable stratification and radial symmetry characteristic of Gulf Stream rings.

We wish to solve (18.32)–(18.34) for the streamfunction $\psi(r, z, t)$, first for $\beta = 0$, assuming $w_E(0) = 0$, $w_E(-H) = (D_E/2)\nabla^2\psi(r, -H, t)$, and the initial condition $\psi(r, z, 0) = \psi_0(r, z)$. The nonlinearities vanish because of

the radial symmetry. Taking a Fourier-Bessel transform of the streamfunction

$$\hat{\psi}(k, z, t) = \int_0^\infty r dr J_0(rk) \psi(r, z, t),$$

we find

$$\left(\frac{\partial}{\partial z} \frac{1}{S} \frac{\partial}{\partial z} - k^2 \right) \psi(k, z, t) = \left(\frac{\partial}{\partial z} \frac{1}{S} \frac{\partial}{\partial z} - k^2 \right) \hat{\psi}_0(k, z),$$

$$\hat{\psi}_{z,t}(k, 0, t) = 0,$$

$$\hat{\psi}_{z,t}(k, -H, t) = \frac{1}{2} k^2 D_E f_0 S(-H) \hat{\psi}(k, -H, t).$$

Solving for $\hat{\psi}$ we obtain

$$\hat{\psi}(k, z, t) = \hat{\psi}_0(k, z) - \hat{\psi}_0(k, -H) F(z; k) (1 - e^{-\sigma(k)t}),$$

where $F(z; k)$ satisfies

$$\frac{\partial}{\partial z} \frac{1}{S} \frac{\partial}{\partial z} F = k^2 F,$$

$$F_z(0; k) = 0,$$

$$F_z(-H; k) = 1,$$

and the inverse spin-down time is given by

$$\begin{aligned} \sigma(k) &= -k^2 D_E f_0 S(-H) / 2 F_z(-H; k) \\ &= [-k^2 S(-H) H / F_z(-H; k)] \sigma_{BT} \end{aligned}$$

where $\sigma_{BT} = f_0 D_E / 2H$ is the inverse barotropic spin-down time. Thus the inverse baroclinic spin-down time is simply related to σ_{BT} by the factor H divided by the penetration depth.

For large scales, the motion spins down uniformly throughout the whole column with $\sigma \approx \sigma_{BT}$. For small scales, the spin-down occurs only over a depth H_R and is much more rapid. We expect, therefore, that the smaller scales will disappear from the deep ocean, perhaps leaving a thermocline signal behind, while the larger scales will decay more slowly but also more completely. In figure 18.12, we show the structures $F(z; k)$ and inverse spin-down times $\sigma(k)$ for various scales $1/k$. Absolute decay rates depend upon D_E —for $D_E = 20$ m, the time scale $\sigma_{BT}^{-1} = 89$ days, so that everything happens in a few months.

For application to rings we assume $\psi_0(r, -H) = -l e^{-(1/2)(r^2/l^2 - 1)} \times 10 \text{ cm s}^{-1}$, which gives maximum currents of 10 cm s^{-1} at a radius l . We solve for the net change in azimuthal velocity $\psi_r(r, z, t \rightarrow \infty) - \psi_{0,r}(r, z)$ and contour this change in figure 18.13. It is seen that the changes in the thermocline and shallow water are negligible so that the persistence of oceanic thermocline eddies is quite consistent with theoretical expectations.

When the beta effect is included, important differences occur in the spin-down of linear eddies. The simplest case to analyze is for weak friction. Then

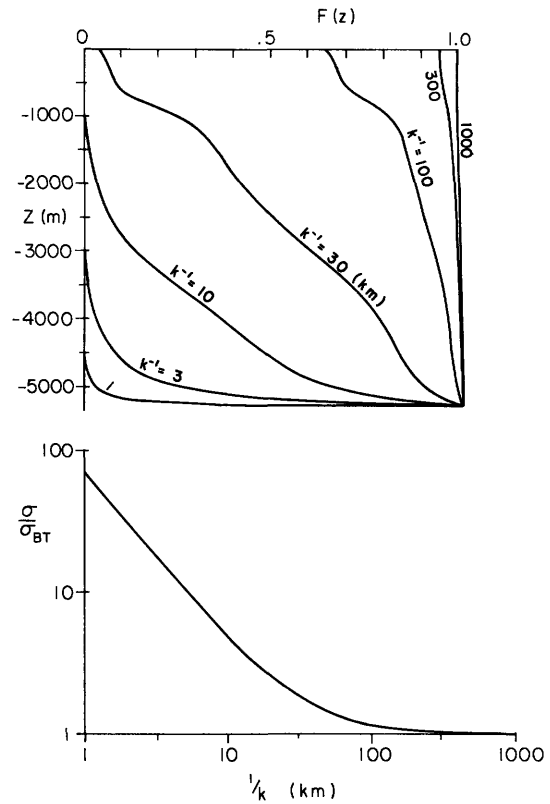


Figure 18.12 Decay in currents F as a function of depth for different radial scales k^{-1} . Actual change is given by $-F(z) \times$ bottom currents. Lower figure shows ratio of decay rate to spin-down rate for a homogeneous fluid as a function of the radial scale.

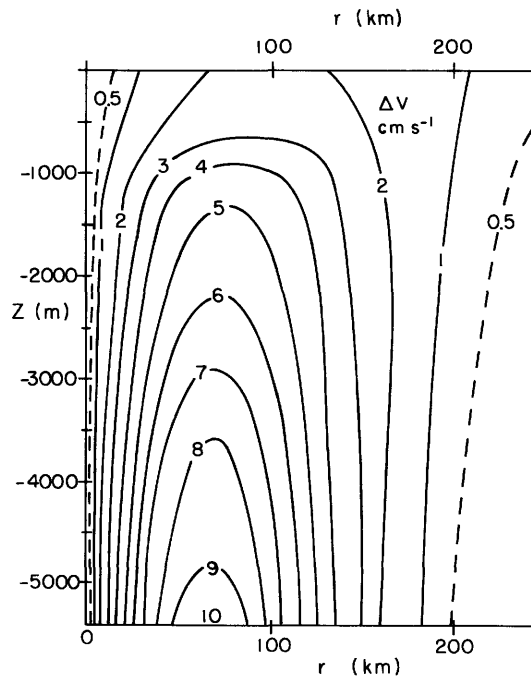


Figure 18.13 Decrease in azimuthal velocity due to bottom friction when initial bottom currents are $10 \text{ cm s}^{-1} (r/l) \times \exp[-\frac{1}{2}(r^2/l^2) + \frac{1}{2}]$.

there are two time scales—the period and the spin-down time. The Fourier–Bessel component with wave-number k and (initially) vertical normal mode $F_n(z)$ behaves like

$$\hat{\psi}_n(k, t) = \hat{\psi}_n(k, 0) F_n(z) / J_0 \left(k \sqrt{\left(x + \frac{\beta t}{k^2 + \lambda_n^2} \right)^2 + y^2} \right) \\ \times \exp[-\sigma_{BT} F_n^2(-H) k^2 t / (k^2 + \lambda_n^2)].$$

This follows from the fact that when the solution of (18.33) is expanded in powers of period/spin-down time, the lowest order component is just a steadily propagating Bessel-function eddy. The next-order component has an inhomogeneous boundary condition due to friction and an inhomogeneous forcing of the equations of motion due to the slow time dependence. Multiplying this first-order equation of motion by $F_n(z)$ and depth averaging shows that the slow time dependence satisfies a simple exponential decay law (see also Flierl, 1978).

One important feature of this solution is the fact that baroclinic modes decay more slowly than barotropic modes both because of the increase in λ_n^2 and because of the appearance of the factor $F_n^2(-H)$. Thus a first-mode deformation-scale eddy with $F_1(-H) = -0.6$ and $k = \lambda$ has a decay rate of $0.2\sigma_{BT}$. But the important feature is that the β -plane eddy, unlike the f -plane eddy, decays completely. The β -effect permits transmission of energy downward, where it can be dissipated by friction. It appears that nonlinearity can impede this process because it slows down the dispersion of a ring (McWilliams and Flierl, 1979).

18.7 Nonlinear Motions

In this section, we shall consider mesoscale flows for which the advection of relative vorticity or density anomaly is important. This can occur either in the form of wave–wave interactions or wave–mean flow interactions. In both cases we are considering motions in which there are significant nonlinear interactions among various scales. This situation is to be contrasted with that in section 18.5.3, in which the mean flow provided a variable environment for the waves but was passive in the sense that there was no exchange of energy between the waves and the mean flow.

18.7.1 Baroclinic and Barotropic Instabilities

The problem of the instability of large-scale atmospheric motions has a long history, going back as always to Helmholtz (1888). The discoveries of the polar front and the polar-front wave by J. Bjerknes (1919) and J. Bjerknes and H. Solberg (1921, 1922) initiated several investigations of the instability of a polar-front model, notably by H. Solberg (1928) and by N. Kotschin (1932).

These studies were incomplete: Solberg's avoided considering the effects of the frontal intersection with ground; Kotschin's considered various possible perturbation modes but not that of the all important baroclinic instability. E. Eliassen (1960) conducted a numerical study of a problem similar to Kotschin's, but with a vertical wall. However, the detailed exploration of Kotschin's model, a front between two fluids of different uniform densities and zonal velocities intersecting upper and lower horizontal boundaries, was left to Orlanski (1968), who considered all the four different instability modes—Helmholtz instability of vertical shear coupled with gravitational stability, Rayleigh instability of horizontal shear, baroclinic instability, and mixed baroclinic–barotropic–Helmholtz instability. Attempts to explain the long atmospheric waves observed in the troposphere were initiated by the work of J. Bjerknes (1937) to which we have already referred. Mathematical theories for the instability of a baroclinic zonal current with uniform horizontal temperature gradients were presented by Charney (1947), Eady (1949), Fjørtoft (1950), Kuo (1951), Green (1960), Burger (1962), Stone (1966, 1970) and many others—the problem is still being investigated. The stability of a horizontally shearing zonal current in two-dimensional spherical flow was studied by Kuo (1949). The stability of flows with both vertical and horizontal shear was investigated by Stone (1969), McIntyre (1970), Simmons (1974), Gent (1974, 1975) and Killworth (1980). The last named is the most comprehensive. Integral conditions for instability in more or less arbitrary zonal flows were developed by analogy with Rayleigh's condition for two-dimensional parallel flows by Kuo (1951), Charney and Stern (1962), Pedlosky (1964a, 1964b), Bretherton (1966a, 1966b), and others.

On the oceanic side, the onset of meandering of the western boundary currents has been dealt with by Orlanski (1969) and Orlanski and Cox (1973). They conclude that the meandering of the Gulf Stream between Miami and Cape Hatteras can be attributed to baroclinic instability, a result which seems to be in agreement with observations of Webster (1961a). The baroclinic instability of the free Gulf Stream extension implies a northward heat transport by the meanders and cutoff vortices. Evidence for such transports is not conclusive. The discovery of the mid-ocean mesoscale eddies initiated attempts by Gill, Green, and Simmons (1974) and Robinson and McWilliams (1974) to ascertain whether these eddies could be ascribed to baroclinic instabilities of the mid-ocean mean flows. The results have not been encouraging. Studies of the behavior of numerical ocean models also do not support this idea (Harrison and Robinson, 1978). If one merely converts available potential energy to kinetic energy while preserving the total energy density per unit area, the perturbation kinetic energies cannot exceed those

of the mean flow, and are therefore too small by an order of magnitude. Only ad hoc energy-convergence mechanisms give the right magnitudes.

Most of the studies referred to above have dealt with the instability of a zonal current with horizontal and/or vertical shear. Realistically, we must also be concerned with the instability of nonzonal and time-dependent flows, including oceanic gyres, forced and free Rossby waves and waves over topography. Thus we need to consider more general basic states.

We begin with the quasi-geostrophic potential vorticity equations (18.33)–(18.35). We attempt to find a basic solution $\bar{\psi}(x, y, z, t)$ and investigate the growth of small perturbations $\psi'(x, y, z, t)$ around this basic state. The most straightforward basic state is a steadily translating (possibly at zero speed) unforced, nondissipative flow field

$$\bar{\psi} = \bar{\psi}(x', y, z), \quad x' = x - \bar{c}t,$$

which satisfies the equations

$$\nabla^2 \bar{\psi} + \frac{\partial}{\partial z} \frac{1}{S} \frac{\partial}{\partial z} \bar{\psi} + \beta y = P(\bar{\psi} + \bar{c}y, z) \quad (18.51)$$

and the boundary conditions

$$\begin{aligned} \bar{\psi}_z(x', y, 0) &= T_s(\bar{\psi} + \bar{c}y), \\ \bar{\psi}_z(x', y, -H) + f_0 S(-H)b(x' + \bar{c}t, y) \\ &= T_b(\bar{\psi} + \bar{c}y). \end{aligned} \quad (18.52)$$

Clearly such a solution is possible only if $\bar{c}b_x = 0$, that is, if the basic flow is independent of time or if the zonal variation in topography vanishes—waves cannot translate over varying topography without changing amplitude or shape. The basic flow is stationary in the x', y, z system and in this system the pseudopotential vorticity is constant along streamlines.

The derivation of (18.51) and (18.52) may indicate that the restrictions upon the mean flow are quite severe—no forcing or dissipation. However, our subsequent derivations will require only (18.51) and (18.52) and these can hold in much more general conditions. For example, the standard meteorological problem considers the instability of zonal flows forced by heating and perhaps Reynolds stresses and dissipated by radiation and surface Ekman pumping. Since both the mean flow and the potential vorticity are functions only of y , we can still define potential vorticity and surface functionals from (18.51)–(18.52). As long as the forcing and dissipative processes are not significant in the perturbation dynamics, the formalism below will apply. (We warn, however, that when there is topography or lateral boundaries, the stability problem for forced and dissipated flow may be quite different.)

The perturbation streamfunction $\psi' = \psi'(x', y, z, t)$ satisfies

$$\begin{aligned} \frac{\partial}{\partial t} \left(\nabla^2 + \frac{\partial}{\partial z} \frac{1}{S} \frac{\partial}{\partial z} \right) \psi' \\ + (\bar{v} - \bar{c}\bar{x}) \cdot \nabla \left(\nabla^2 + \frac{\partial}{\partial z} \frac{1}{S} \frac{\partial}{\partial z} - P' \right) \psi' = 0, \end{aligned} \quad (18.53a)$$

$$\begin{aligned} P'(\Psi, z) &= \frac{\partial}{\partial \Psi} P(\Psi, z), \\ \frac{\partial}{\partial t} \psi'_z + (\bar{v} - \bar{c}\bar{x}) \cdot \nabla \left(\frac{\partial}{\partial z} - T' \right) \psi' &= 0, \end{aligned} \quad (18.53b)$$

$$z = 0, -H.$$

If we examine the normal modes $\psi'(x, y, z, t) = \psi'(x', y, z) e^{\sigma t}$, we have the eigenvalue equation for the growth rate

$$\begin{aligned} \sigma \left(\nabla^2 + \frac{\partial}{\partial z} \frac{1}{S} \frac{\partial}{\partial z} \right) \psi' \\ = -(\bar{v} - \bar{c}\bar{x}) \cdot \nabla \left(\nabla^2 + \frac{\partial}{\partial z} \frac{1}{S} \frac{\partial}{\partial z} - P' \right) \psi', \end{aligned} \quad (18.54a)$$

with boundary conditions

$$\begin{aligned} \sigma \psi'_z &= -(\bar{v} - \bar{c}\bar{x}) \cdot \nabla \left(\frac{\partial}{\partial z} - T'_s \right) \psi', \quad z = 0, \\ \sigma \psi'_z &= -(\bar{v} - \bar{c}\bar{x}) \cdot \nabla \left(\frac{\partial}{\partial z} - T'_b \right) \psi', \quad z = -H. \end{aligned} \quad (18.54b)$$

These equations for the perturbation streamfunction ψ' and the growth rate σ will form the basis for discussion of zonal flow instability and wave instabilities below.

Integral Theorems The classic example of an integral theorem is, of course, the Rayleigh theorem (1880). However, there is a slightly more general theorem, due originally to Arnol'd (1965) and applied to quasi-geostrophic flow by Blumen (1968), which we shall extend here to the problem of traveling disturbances and/or stationary motion over topography. This theorem states that the flow is *stable* if the potential vorticity and buoyancy along the bottom surface increase, and the buoyancy along the top surface decreases, with increasing streamfunction, that is, $P' \geq 0$, $T'_s \leq 0$, $T'_b \geq 0$ everywhere. To prove this, let us assume that $P' > 0$, $T'_s < 0$, and $T'_b > 0$ everywhere. (The cases for $P' = 0$ or $T'_s = 0$ or $T'_b = 0$ everywhere are readily proved.) First, we form an energy equation by multiplying (18.54a) by $-\psi'^*$, volume integrating, adding the conjugate equation, integrating by parts, and applying the boundary conditions. We obtain

$$\begin{aligned} (\sigma + \sigma^*) \iiint |\nabla \psi'|^2 + \frac{1}{S} |\psi'_z|^2 \\ = \iiint q' J(\bar{\psi} + \bar{c}y, \psi'^*) + \text{c.c.} + \iint \psi'_z J(\bar{\psi} + \bar{c}y, \psi'^*) \\ + \text{c.c.} \Big|_{-H}^0. \end{aligned} \quad (18.55)$$

Next, we form a normalized enstrophy equation by multiplying (18.54a) by q'^*/P' (recalling that $P' \neq 0$) and volume integrating to get

$$(\sigma + \sigma^*) \iiint \frac{|q'|^2}{P'} = - [\iiint q'^* (\bar{\psi} + \bar{c}y, \psi') + \text{c.c.}] \quad (18.56)$$

Applying a similar procedure to the upper and lower boundary conditions, adding the result to (18.55) and (18.56), gives

$$(\sigma + \sigma^*) \iiint \left[|\nabla\psi'|^2 + \frac{1}{S} |\psi'_z|^2 + \frac{1}{P'} |q'|^2 - \frac{1}{H} \frac{1}{T'_s S(0)} |\psi'_z(0)|^2 + \frac{1}{HT'_b S(-H)} |\psi'_z(-H)|^2 \right] = 0. \quad (18.57)$$

For the choice $P' > 0$, $T'_s < 0$, and $T'_b > 0$ the integrand is positive definite, implying that $\text{Re}(\sigma) = 0$, that is, that the flow is stable. When P' , T'_s , or T'_b are everywhere zero, the enstrophy or surface-temperature variance equations simply show that $|q'|$ or $|\psi'_z|$ at 0 or $-H = 0$, so that the term contributing to (18.55) can be ignored and therefore will also not enter in (18.57).

This completes the proof of the theorem. From the relation between the potential vorticity and the streamfunction (in the moving coordinate system) and the relation between the surface buoyancies and the streamfunctions at the top and bottom surfaces, we can tell whether the flow is stable or potentially unstable. In some problems (cf. Howard, 1964b; Rosenbluth and Simon, 1964) the necessary criterion for stability has been shown to be sufficient. We should also mention that the normal-mode assumption is not essential, so that the theorem applies to an arbitrary initial disturbance (Blumen, 1968).

In illustration, we note that the theorem implies that the Fofonoff (1954) inertial gyre solution,

$$P(\bar{\psi}) = \alpha\bar{\psi}, \quad T_s(\bar{\psi}) = T_b(\bar{\psi}) = 0, \quad \bar{c} = 0,$$

where α is a positive constant, is stable, as first pointed out by McWilliams (1977). We could find many other stable gyres by numerical means, including topographical effects, by solving (18.51), (18.52) with arbitrary functionals P and $T_{s,b}$ constrained only to satisfy the proper derivative conditions. The simplest would be to take

$$P(\bar{\psi}, z) = a(z)\bar{\psi} + b(z),$$

with $a(z) > 0$ and similar linear functionals for the boundary conditions.

A second example is the flow forced by Gulf Stream meandering described in section 18.5.3. In this case, the potential vorticity equation for the forced wave (the basic state) is

$$\nabla^2\psi + \beta y = P(\bar{\psi} + \bar{c}y).$$

The substitutions

$$\bar{\psi} = \Psi_0 e^{-\nu y} e^{i(kx - \omega t)}$$

and

$$\bar{c} = \omega/k$$

show that $P(Z) = \beta Z/\bar{c}$. Therefore, when the forcing propagates eastward, the trapped wave is *stable*. Unlike ordinary propagating Rossby waves, for which $\bar{c} < 0$, and which Lorenz (1972) has shown to be unstable, forced waves may be stable. We shall consider topographically forced waves in detail in section 18.7.3.

Zonal Flows We now specialize to zonal flows $\bar{\psi} = -\int^y \bar{u}(y', z) dy'$, $b_x = 0$. For these, we can readily find P' and $T'_{s,b}$ by taking y derivatives of (18.51) and (18.52):

$$P' = (\beta - \bar{u}_{yy} - \frac{\partial}{\partial z} \frac{1}{S} \frac{\partial}{\partial z} \bar{u}) / (\bar{c} - \bar{u}),$$

$$T'_s = -\bar{u}_z / (\bar{c} - \bar{u})|_{z=0},$$

$$T'_b = (f_0 S b_y - \bar{u}_z) / (\bar{c} - \bar{u})|_{z=-H},$$

where \bar{c} now is completely arbitrary (i.e., the perturbation wave speed will be simply doppler shifted by \bar{c}). In particular, we can choose \bar{c} so that $\bar{c} - \bar{u}$ has a definite sign. Therefore we see that the flow will be stable if all the three quantities

$$\beta - \bar{u}_{yy} - \frac{\partial}{\partial z} \frac{1}{S} \frac{\partial \bar{u}}{\partial z},$$

$$\bar{u}_z(0),$$

$$f_0 S(-H) b_y - \bar{u}_z(-H)$$

have the same sign. Thus we recover the generalized Rayleigh theorem for quasigeostrophic flows: the flow is stable if

$$\begin{aligned} \bar{Q}_y = & \beta - \bar{u}_{yy} - \frac{\partial}{\partial z} \frac{1}{S} \frac{\partial \bar{u}}{\partial z} + \frac{\bar{u}_z}{S} \delta(z) \\ & + \left(f_0 b_y - \frac{\bar{u}_z}{S} \right) \delta(z + H) \end{aligned} \quad (18.58)$$

is uniform in sign (δ is the Dirac delta function). More conventional proofs of this theorem also can be found in Charney and Stern (1962), Pedlosky (1964a), and Bretherton (1966b).

A second standard theorem in shear flow instability theory due to Fjörtoft (1950) can also be generalized to the quasi-geostrophic flow problem. If we suppose that \bar{Q}_y vanishes along some curve in the (y, z) plane and furthermore that $\bar{u} = \bar{u}_c = \text{constant}$ on this curve, the flow will be stable if $\bar{Q}_y(\bar{u} - \bar{u}_c)$ is negative everywhere. This can be demonstrated by choosing $\bar{c} = \bar{u}_c$. Clearly the requirement that $\bar{u} = \bar{u}_c$ at all points where

$$\beta - \bar{u}_{yy} - \frac{\partial}{\partial z} \frac{1}{S} \frac{\partial}{\partial z} \bar{u} = 0$$

is highly restrictive (though it does occur for $\bar{u}_y = 0$ or $\bar{u}_z = 0$ or $\bar{u}_{yy} + (\partial/\partial z)(1/S)(\partial/\partial z)\bar{u} = K\bar{u}$).

As a practical application, we remark that the Rayleigh theorem (18.58) implies that the Eady (1949) problem ($S = \text{constant}$, $\bar{u}_z = \text{constant}$, $\beta = 0$, $\bar{u}_y = 0$) can be stabilized by a sloping topography such that $b_y > \bar{u}_z/f_0S|_{-H}$. This slope is steeper than the isopycnal slope, so that the density gradient at the bottom becomes opposite in sign to the gradient at the surface.

A second application is to demonstrate the stabilizing effort of β , especially for eastward flows. We consider zonal currents with a barotropic plus a sheared flow with the structure of the flat-bottom first-baroclinic mode

$$\bar{u}(y,z) = \bar{u}_{BT} + \bar{u}_{BC}F_1(z)$$

with \bar{u}_{BT} and \bar{u}_{BC} constants. (Many currents in the ocean do seem to have dominantly first-mode shears.) The Rayleigh criterion becomes

$$\bar{Q}_y = \beta + \frac{\bar{u}_{BC}}{L_R^2} F_1(z) > 0$$

for all z . This can occur only if

$$-\frac{\beta L_R^2}{|F_1(0)|} < \bar{u}_{BC} \equiv \frac{\Delta u}{|F_1(0)| + |F_1(-H)|} < \frac{\beta L_R^2}{|F_1(-H)|}$$

where Δu is the change in velocity from bottom to top. Using our N^2 profile this implies

$$-4 \text{ cm s}^{-1} < \Delta u < 22 \text{ cm s}^{-1}.$$

We see that eastward currents are considerably more stable than westward flows. Gill, Green and Simmons (1974) report on calculations which show weak growth rates for $\Delta \bar{u} \sim -5 \text{ cm s}^{-1}$. Observations of actual $\Delta \bar{u}$'s are not readily available because the midocean density-field measurements are generally contaminated with eddies. However, it is not unlikely that mid-ocean mean currents away from the "recirculation region" of Worthington (1976) (see also chapters 1 and 3) are smaller than this magnitude, so that mid-ocean flows may very possibly be stable (see also McWilliams, 1975).

This result must be viewed with caution, because it is possible for forced meridional currents to be locally unstable for any value of the shear. We can see this by considering the stability of a mean flow

$$\bar{\psi} = \bar{v}(z)x - \bar{u}(z)y,$$

where we ignore the dynamics of the mechanism that supports the \bar{v} component of flow on the grounds that its space and time scales are much larger than those of the perturbations we wish to consider. The perturbations satisfy

$$\frac{\partial}{\partial t} q' + J(\bar{\psi}, q') + J(\psi', \bar{q}) = 0,$$

where

$$\bar{q} = \left(\frac{\partial}{\partial z} \frac{1}{S} \frac{\partial}{\partial z} \bar{v} \right) x + \left(\beta - \frac{\partial}{\partial z} \frac{1}{S} \frac{\partial}{\partial z} \bar{u} \right) y$$

is now *not* expressible as $P(\bar{\psi}, z)$. However, we may consider perturbations of the form

$$\psi' = F(z) \exp[ik(x - ct) + ily]$$

to find

$$\left[(\bar{u} - c) + \frac{l}{k} \bar{v} \right] \left(\frac{\partial}{\partial z} \frac{1}{S} \frac{\partial}{\partial z} - k^2 - l^2 \right) F + \left[\beta - \frac{\partial}{\partial z} \frac{1}{S} \frac{\partial}{\partial z} \left(\bar{u} + \frac{l}{k} \bar{v} \right) \right] F = 0.$$

Applying the usual Rayleigh theorem shows that the flow will be stable unless $\beta - (\partial/\partial z)(1/S)(\partial/\partial z)[\bar{u} + (l/k)\bar{v}]$ changes sign. If $\bar{v} \neq 0$, however, a proper choice of l and k (the direction of the perturbation wave) may always be made to ensure satisfying the necessary criterion for instability. Thus arguments about the zonal flow stability may not directly apply to the Sverdrup circulation.

The discussion of baroclinic instability has been extended to finite amplitudes by Lorenz (1962, 1963a) using truncated spectral expansions and by Pedlosky (1970, 1971, 1972, 1976, 1979b), Drazin (1970, 1972), and others using expansion techniques in the vicinity of critical values of the stability parameters. Thus far, the systems dealt with have been more applicable to laboratory models than the actual atmosphere or ocean. A general review has been given by Hart (1979a), who himself has contributed by experiment and analysis to the subject.

18.7.2 Wave-Mean Flow Interactions

The subject of wave-mean flow interaction in the atmosphere has been treated extensively in connection with the manner in which large-scale waves generated in the troposphere propagate vertically into the stratosphere and there interact with the mean flow. One example is the so-called sudden-warming phenomenon, the rapid breakdown of the stratospheric winter circumpolar cyclone accompanied by large-scale warming. Another example is the so-called quasi-biennial oscillation, which has been explained as a wave-mean flow interaction between vertically propagating Rossby-gravity and Kelvin waves and the zonal flow in the equatorial stratosphere (Lindzen and Holton, 1968; Holton and Lindzen, 1972). A vivid experimental and theoretical demonstration of this type of interaction has been given by Plumb and McEwan (1978).

Charney and Drazin (1961) have shown that small-amplitude steady waves in quasi-geostrophic, adiabatic, inviscid flow cannot interact to second order with the zonal flow. If there are no critical surfaces at which the zonal flow vanishes and there is no dissipation, forcing, or transience, no interaction will take place. All are present in the quasi-biennial oscillation and in Plumb and McEwan's model. The result of Charney and Drazin was originally derived by straightforward calculation. It may also be inferred from an independent study of energy transfer in stationary waves by Eliassen and Palm (1960), who derive linear relations between the horizontal Reynolds stress, the horizontal eddy heat flux, and the components of the wave energy flux. These works have been greatly extended by Andrews and McIntyre (1976), Boyd (1976), and Andrews and McIntyre (1978a,b). McIntyre (1980) reviews the subject.

There have been several suggestions of oceanic analogies: Pedlosky (1965b) and N. Phillips (1966b) have argued that westward-propagating Rossby waves can cause acceleration of the western boundary currents. Lighthill (1969) attempted to explain the onset of the Somali Current as due to the interaction of Rossby-gravity waves generated by the monsoon winds in the mid-Indian Ocean with the flow in the vicinity of the East African continent. More recently, experiments of Whitehead (1975) have shown quite clearly that mean flows may be generated by radiated Rossby waves. His work led Rhines (1977) to a theoretical reconsideration of the wave-mean flow generation problem not only when the geostrophic contours (the f/H lines which represent the streamlines for free inertial motions) are closed or periodic but also when the contours are open. Rhines's work is important for understanding large-scale forced motions in oceanic basins.

As an illustration of wave-mean flow interaction in an oceanographic context we shall ask again whether the waves produced by Gulf Stream meandering may be responsible for generating and maintaining the so-called recirculation flow found by Worthington (1976) and others. This flow occurs in a region extending some 1000 km south of the stream and contains (according to Worthington) a sizable westward transport ($10^8 \text{ m}^3 \text{ s}^{-1}$). This problem has been addressed by Rhines (1977), who, however, did not consider generation due to eastward-moving waves.

We consider the barotropic flow south of the Gulf Stream forced by the streamfunction $\psi(x,0,t) = A \cos(kx - \omega t)$, as in section 18.5.3, but we now include the effects of bottom Ekman friction and the second-order interaction with the mean zonal flow. The streamfunction satisfies

$$\left(\frac{\partial}{\partial t} + \sigma_{\text{BT}}\right) \nabla^2 \psi + \beta \psi_x = -f(\psi, \nabla^2 \psi),$$

$$\psi(x,0,t) = A \cos(kx - \omega t),$$

$$\psi \rightarrow 0, \quad y \rightarrow -\infty.$$

The linear solution (assuming Ak^3/β small) will be

$$\psi = \text{Re}\{A \exp[i(kx - \omega t) + \nu y]\},$$

$$\nu = \sqrt{k^2 + \beta\omega/(\omega^2 + \sigma_{\text{BT}}^2) - i\beta k\sigma_{\text{BT}}/(\omega^2 + \sigma_{\text{BT}}^2)},$$

if the root with positive real part is chosen to satisfy the radiation condition. The nonlinearly forced streamfunction field satisfies

$$\left(\frac{\partial}{\partial t} + \sigma_{\text{BT}}\right) \nabla^2 \psi^{(1)} + \beta \psi_x^{(1)} = -2A^2 \nu_r \nu_i k e^{2\nu_r y}$$

where ν_r and ν_i are the real and imaginary parts of ν , respectively. Its solution is

$$\psi^{(1)} = -\frac{A^2 \nu_i k}{2\sigma_{\text{BT}}} e^{2\nu_r y}$$

or

$$\bar{u} = \frac{A^2 \nu_r \nu_i k}{\sigma_{\text{BT}}} e^{2\nu_r y}.$$

This is, of course, just the solution to

$$\sigma_{\text{BT}} \bar{u} = -(\bar{u}'v')_y$$

with u' and v' taken from the lowest-order solution.

The mean flow is determined by a balance between friction and Reynolds-stress forcing. The importance of dissipation becomes clear: without friction, ν is either purely real or purely imaginary and $\bar{u} = 0$. With friction, we find that the waves transfer momentum into the mean flow. Moreover, we can show that the magnitude of the flow is not sensitive to the spin-down time $1/\sigma_{\text{BT}}$, as this time becomes very large.

As σ_{BT} becomes small we find

$$\nu \approx \begin{cases} \sqrt{k^2 + \frac{\beta k}{\omega}} - i\beta\sigma_{\text{BT}}k/2\omega^2 \sqrt{k^2 + \frac{\beta k}{\omega}}, & \frac{\omega}{k} > 0, \\ \omega/k < -\beta/k^2 \\ -i\sqrt{-k^2 - \frac{\beta k}{\omega}} + \beta\sigma_{\text{BT}}k/2\omega^2 \sqrt{k^2 - \frac{\beta k}{\omega}}, & \\ -\beta/k^2 < \omega/k < 0. \end{cases}$$

The forced mean flow is therefore

$$\bar{u} = -\frac{\beta A^2 k^2}{2\omega^2} \begin{cases} \exp\left(2\sqrt{k^2 + \frac{\beta k}{\omega}} y\right), & \frac{\omega}{k} > 0, \\ \omega/k < \beta/k^2 \\ \exp\left(\beta\sigma_{\text{BT}}ky/\omega^2 \sqrt{-k^2 - \frac{\beta k}{\omega}}\right), & \\ -\beta/k^2 < \omega/k < 0, \end{cases}$$

with amplitude independent of σ_{BT} . We can estimate the westward current speeds by relating the amplitude A to the excursions of the stream in the y direction:

$$d = -A \frac{k}{\omega} \cos(kx - \omega t) \equiv d_0 \cos(kx - \omega t).$$

The maximum westward currents are $-\frac{1}{2}\beta d_0^2$. Rhines (1977) has derived from more general considerations the result that mean-flow generation is proportional to β times the square of the displacement. For typical excursions of 100–200 km, mean flows of 10–40 cm s^{-1} can be generated. [We should note that, for this problem, the eastward Stokes drift is given by

$$A^2 \frac{k}{\omega} \left(k^2 + \frac{\beta k}{\omega} \right) \exp \left(2 \sqrt{k^2 + \frac{\beta k}{\omega}} y \right),$$

which is larger than the westward Eulerian flow so that the particle drift is *eastward*.]

Observations of Gulf Stream meanders usually indicate eastward-moving disturbances; therefore much of the mean flow will be trapped in a distance one-half that shown in figure 18.12. The disturbances that generate propagating waves ($-\beta/k^2 < \omega/k < 0$) can produce mean flows over large north–south distances, but there does not seem to be enough amplitude in such disturbances. (See, however, the remarks in section 18.8)

This very simple calculation indicates that eddy radiation from the meandering Gulf Stream can generate a return flow with speeds comparable to those suggested by observations (cf. Worthington, 1976; Wunsch, 1978a; Schmitz, 1977; see also chapter 4). The predicted north–south scale of the region is quite small, however, unless there is considerably more energy in westward-going meanders than has been suggested by Hansen (1970) or by Robinson, Luyten, and Fuglister (1974).

There is another form of wave–mean flow interaction involving overreflection of waves traveling through a variable mean-flow field. Lindzen and Tung (1978) recently have demonstrated that barotropic and baroclinic instabilities may be explained as overreflection phenomena in which Rossby waves impinging upon a critical surface are reflected with a coefficient of reflection greater than unity. The combination of an overreflecting region in the mean flow with a reflecting boundary can lead to a growing disturbance in which the wave picks up energy at each passage into the overreflecting region.

This concept may be directly applicable to the problem of reflection of Rossby waves from the western boundary currents.⁶ Numerous examples of Gulf Stream rings interacting with the Gulf Stream without being absorbed can be found in the data presented by Lai and Richardson (1977), and at times they appear to increase in energy as a result of the interaction (Richardson, Cheney, and Mantini, 1977). We suggest the

possibility that overreflection may be involved in the dynamics of mesoscale eddies near the western boundary current. Whether or not this is so remains to be seen.

18.7.3 Wave Instability and Form-Drag Instability

The fact that Rossby waves may be unstable was first shown by Lorenz (1972) for a barotropic atmosphere. In a more detailed exploration of the problem Gill (1974) observed that there are two distinct mechanisms for the instability: a resonant triad interaction or a shear instability of the Rayleigh type. Duffy's (1978) and Kim's (1978) baroclinic studies showed that baroclinicity may also cause instability in large-scale waves. As in the instability of zonal flow, the growing baroclinic modes have the scale of the radius of deformation. Jones (1978) and Fu and Flierl (1980) have explored these ideas further as they apply to the ocean.

Wave and Form-Drag Instabilities Just as a freely propagating wave provides variations of potential vorticity which may lead to instability, topography may produce a forced flow whose variations of potential vorticity may also cause instability. Topography may be a destabilizing influence, either because the forced flow is unstable, just as a free wave, to Rayleigh or resonant instabilities, or else because the topography itself may help—via the form drag produced by the perturbation—to extract energy from the mean flow. The latter type of instability was first encountered by Charney and DeVore (1979) in their study of blocking (the persistence of anomalously high pressure in certain regions of the atmosphere) in a barotropic atmosphere. In their model, blocking occurs as an alternative flow equilibrium corresponding to a given forcing of the zonal flow in the presence of sinusoidal topography. It was found that the transition from the normal flow state to the anomalous blocking state takes place via a form-drag instability of an intermediate equilibrium state in which the zonal flow is superresonant. In this superresonant state, a small decrease of the zonal flow amplifies the forced orographic wave and increases the form drag (mountain torque), which in turn decelerates the zonal flow still further. Charney and Straus (1980) extended this study to a two-layer baroclinic atmosphere. Here again there is a form-drag instability. But when there is no lower layer flow, the instability is catalyzed by the form drag: the perturbation derives its energy from the available potential energy of the Hadley circulation generated by thermal forcing; the form drag merely establishes the necessary phase relationships.

The connections between this form-drag instability and the more familiar resonant or Rayleigh instabilities have not been previously explored. For this purpose, consider the simplest wavelike flow of a homogeneous

ocean and derive the instability conditions for both a free zonally propagating wave and a topographically forced Rossby wave in order to elucidate the similarities and differences among the respective instability mechanisms. We begin by stating the forms of the potential vorticity functionals $P(\bar{\psi} + \bar{c}y)$ and the resulting perturbation equations. For the Rossby wave, $\bar{c} = -\beta/k^2$, the potential vorticity functional in equation (18.51) is

$$P(Z, z) = (\beta/\bar{c})Z = -k^2Z$$

with streamfunction

$$\bar{\psi} = A \sin kx.$$

The perturbation equation (18.53a) is particularly simple because P' is now a constant:

$$\sigma \nabla^2 \psi' + J\left(-\frac{\beta}{k^2}y + A \sin kx, (\nabla^2 + k^2)\psi'\right) = 0, \quad (18.59)$$

where A is completely arbitrary.

For barotropic flow over topography of the form $b = b_0 \sin kx$ on the β -plane, the basic state potential vorticity equation

$$\nabla^2 \bar{\psi} + \beta y + \frac{f_0 b_0}{H} \sin kx = P(\bar{\psi})$$

has the solution

$$\bar{\psi} = -\bar{u}y + A \sin kx, \quad A = \frac{\bar{u}f_0 b_0/H}{\bar{u}k^2 - \beta}$$

with the linear potential vorticity functional

$$P(Z) = -\frac{\beta}{\bar{u}}Z \equiv -k_u^2 Z$$

Here k_u is the wavenumber of the stationary wave (k_u^2 may be less than zero). The perturbation equation

$$\sigma \nabla^2 \psi' + J\left[-\frac{\beta}{k_u^2}y + A \sin kx, (\nabla^2 + k_u^2)\psi'\right] = 0 \quad (18.60)$$

is very similar in form to (18.59) except that k and k_u are now independent; however, the amplitude A for the topographical problem is determined by

$$A = \frac{f_0 b_0/H}{k^2 - k_u^2}.$$

Obviously we need only to solve (18.60) and find $\sigma(\beta, A, k, k_u)$; we can then identify both the free ($k_u = k$) and forced ($k_u \neq k$) regimes. In actuality the task is even simpler since dimensional considerations show that there are only two parameters, $M = Ak^3/\beta$ and $\mu = k_u/k$, that must be varied while computing the nondimensional growth rate σ/Ak^2 .

First, however, we demonstrate that only the $k_u^2 > 0$ case need be considered, since the flow is stable for $k_u^2 < 0$. This follows readily from (18.57):

$$(\sigma + \sigma^*) \left(\iint |\nabla \psi'|^2 - \frac{1}{k_u^2} |\nabla^2 \psi|^2 \right) = 0,$$

which implies that Rossby waves $k_u^2 = k^2 > 0$ and waves forced by eastward flow may be unstable, while waves forced by westward flow $k_u^2 < 0$ are definitely stable. Again, as in section 18.7.1 we see that stable waves are generated when the relative motion of the forced wave with respect to the ambient flow is eastward. In addition, for eastward flow over topography or westward-propagating free Rossby waves, a necessary condition for instability is that the perturbation have components with scales larger than k_u^{-1} and components with scales smaller than k_u^{-1} . This follows from Fourier analyzing ψ' and substituting in (18.57) to get

$$\iint d\mathbf{s} |\mathbf{s}|^2 |\hat{\psi}'(\mathbf{s})|^2 \left[1 - \frac{|\mathbf{s}|^2}{k_u^2} \right] = 0,$$

which implies that $|\hat{\psi}'(\mathbf{s})|$ must be nonzero both for some values of $|\mathbf{s}|^2$ larger than k_u^2 and some values smaller than k_u^2 .⁷ This is the perturbation form of Fjørtoft's (1953) result on energy cascades.

We could readily solve the stability problem (18.60) using the mathematical techniques of Lorenz (1972), Gill (1974), Coaker (1977), or Mied (1978) to investigate growth rates. Alternatively we could discuss the limiting behavior—the Rayleigh limit for $M = Ak^3/\beta \gg 1$, the resonant interaction limit for $M \ll 1$, and the form-drag instability—by separate approximations. We shall do this for the last-named problem because it represents a relatively unfamiliar phenomenon. However, to ascertain most clearly the connections between the various types of behavior, it is most simple to employ the Fourier expansion

$$\psi' = e^{i l_0 y} [A_0 e^{i k_0 x} + A_{-1} e^{i(k_0 - k)x} + A_1 e^{i(k_0 + k)x} + \dots]$$

and truncate to the three indicated terms (cf. Gill, 1974). The resulting dispersion relation becomes just

$$\begin{aligned} & (\omega K_{-1}^2 + B_{-1})(\omega K_0^2 + B_0)(\omega K_1^2 + B_1) \\ &= \frac{I_0^2 A^2 k^2}{4} [k_u^2 - K_0^2][(k_u^2 - K_{-1}^2)(\omega K_1^2 + B_1) \\ & \quad + (k_u^2 - K_1^2)(\omega K_{-1}^2 + B_{-1})] \end{aligned} \quad (18.61)$$

using the notation $\omega = i\sigma$, $K_n^2 = (k_0 + nk)^2 + I_0^2$, $B_n = \beta[k_0 + nk](k_u^2 - K_n^2)/k_u^2$. For Rossby waves we simply replace k_u by k .

We have sketched the dependence of $\hat{\sigma} = \sigma/Ak^2$ upon k_0 and I_0 for various M and μ values in figure 18.14. When $M \gg 1$, there is a broad area of (k_0, I_0) space in which the growth rates are real. The maximum occurs for $k_0 = 0$ (this is really a form of Squire's theorem) and

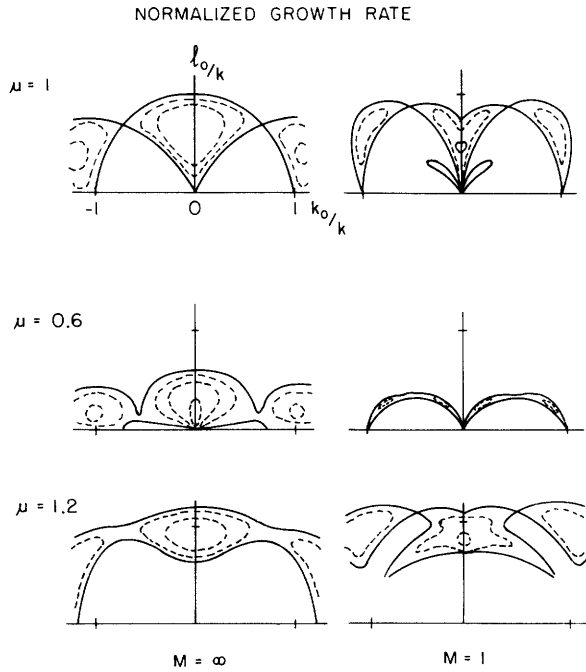


Figure 18.14 Growth rate divided by Ak^2 as a function of k_0 , l_0 for various ratios of the stationary wavenumber to the topographic wavenumber μ and wave steepnesses M . The solid lines are the zero contour. The dashed contours, separated by the interval 0.1, correspond to positive growth rates.

the instability equation is similar to the barotropic instability equation. As M decreases the instability ($\hat{\sigma}$ real) becomes restricted more and more to a band around the frequency resonance line (see below). When μ decreases from 1 to a quantity smaller than 1 ($\bar{u} > \beta/k^2$), the point of maximum growth rate for $M = \infty$ moves to smaller wavenumbers l_0 . For finite M , the same thing occurs—the largest growth rate moves towards $k_0 = l_0 = 0$ as μ decreases. On the other hand, when μ increases from 1 the forced wave becomes stable for small k_0 and l_0 , even for small M , and the wavenumber for maximum growth migrates to smaller scales.

We are thus led to consider the three limits for (18.61):

Strong waves (A or M large): When A is large, the frequency ω is order A and we can neglect all of the B 's to find

$$\sigma = \frac{A|l_0 k|}{2} \sqrt{\frac{-(k_u^2 - K_0^2)[K_1^2(k_u^2 - K_{-1}^2) + K_{-1}^2(k_u^2 - K_1^2)]}{K_0^2 K_1^2 K_{-1}^2}}$$

Clearly the flow will be unstable for $K_0^2 < k_u^2 < K_1^2, K_{-1}^2$; this will always be possible by proper choice of l_0 and k_0 . This is just the Rayleigh instability of the shear flow corresponding to the wave field. The maximum growth rate occurs at $k_0 = 0$:

$$l_0 = \begin{cases} (-1 + \sqrt{\mu^2 + \mu^4})^{1/2}, & \mu > \left(\frac{\sqrt{5}-1}{2}\right)^{1/2} \\ 0, & \mu < \left(\frac{\sqrt{5}-1}{2}\right)^{1/2} \end{cases} \quad (18.62)$$

However, in the topographic case, A can be large not only for very strong topography ($f_0 b_0 k/H \gg \beta$), but also because the zonal flow is nearly critical. In the latter case $\mu \approx 1$, so that the free and forced wave instabilities are indistinguishable. If the flow is not critical, but rather is forced by strong topography, the formula shows the maximum growth rate occurs at $k_0 \rightarrow 0$, $l_0 \rightarrow 0$.

Weak waves (A very small or M small): Here the critical condition is that two of the roots of the left-hand side of (18.61)—for example, $-B_0/K_0^2$ and $-B_1/K_1^2$ —coalesce. This resonance condition

$$B_0/K_0^2 = B_1/K_1^2$$

or

$$\frac{k_0(k_u^2 - K_0^2)}{k_u^2 K_0^2} = \frac{(k_0 + k)(k_u^2 - K_1^2)}{k_u^2 K_1^2}$$

permits the order A part of the frequency to be complex since

$$K_0^2 K_1^2 (\omega + B_0/K_0^2)^2 \approx -\frac{I_0^2 A^2 k^2}{4} (k_u^2 - K_0^2)(k_u^2 - K_1^2)$$

has a complex root for $K_0^2 < k_u^2 < K_1^2$. The growth rate is

$$\sigma = \frac{A|l_0 k|}{2} \sqrt{\frac{(k_u^2 - K_0^2)(K_1^2 - k_u^2)}{K_0^2 K_1^2}}$$

However, the resonance condition must also hold. We can relate this to the more familiar wave-resonance conditions by defining the intrinsic frequencies of the two components of the perturbation and also that of the mean flow by

$$\hat{\omega}_0 = -\beta k_0/K_0^2,$$

$$\hat{\omega}_1 = -\beta(k_0 + k)/K_1^2,$$

$$\hat{\omega} = -\beta k/k_u^2 = -\bar{u}k.$$

The resonance conditions

$$(k_0 + k, l_0) = (k_0, l_0) + (k, 0),$$

$$\hat{\omega}_1 = \hat{\omega}_0 + \hat{\omega}$$

both hold. We show the resonance curves and growth rates for various values of k_u/k in figure 18.15.

For large μ (small mean flow speed), the resonant interaction (except for large l_0) is really a triplet interaction between the two perturbation waves and the topography itself (rather than the forced wave). This is, of course, a stable situation. As μ becomes less than

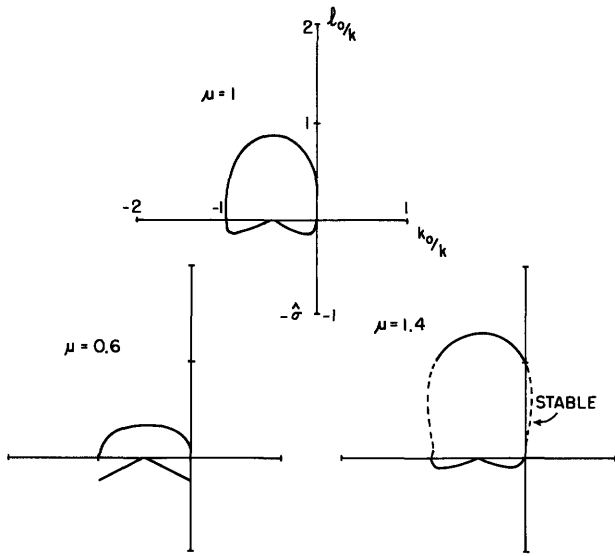


Figure 18.15 Curves above x axis show relation between k_0 and l_0 required by resonance condition. Curves below axis are plots of $-\hat{\sigma}$, showing the dependence of the growth rate upon k_0 .

about 0.9, however, the maximum growth rate again occurs as $k_0 \rightarrow 0$ and $l_0 \rightarrow 0$ [$l_0 \sim (\mu^2 k_0 / 1 - \mu^2)^{1/2}$].

Form-drag instability: Thus in either case we are led to consider what will be shown to be a form-drag instability—the nonzero growth rates occurring at small k_0 and l_0 —when $\mu < 0.79$. There is some difficulty here since the origin is a singularity for M finite; this problem would be eliminated in a bounded geometry. For convenience, we will take the limits $k_0 \rightarrow 0$ first and then $l_0 \rightarrow 0$ since this case has a simple physical interpretation. Applying these limits to (18.61) gives the frequency:

$$\omega^2 = \left[\frac{\beta}{k} \frac{k_u^2 - k^2}{k_u^2} \right]^2 + \frac{A^2 k_u^2}{2} (k_u^2 - k^2). \quad (18.63)$$

The flow is unstable when the right-hand side is negative, which cannot occur for Rossby waves $k_u = k$, but may occur for topographic waves when $k_u < k$ or \bar{u} is greater than the critical speed β/k^2 . In fact, the range is

$$\beta/k^2 < \bar{u} < \beta/k^2 \left(1 + \left[\frac{1}{2} \left(\frac{f_0 b_0}{H} \right)^2 \frac{k^2}{\beta^2} \right]^{1/3} \right).$$

(The resonant triad instability for $\mu < 1$ does not appear here; rather, the limit $k_0 \rightarrow 0^-$ and $l_0 \sim (-k_0)^{1/2} \rightarrow 0^+$ must be used.) So far we have looked at the mathematics; let us now discuss the physics of this instability and also show that the truncation to three terms is valid.

The form-drag instability involves one component A_0 which has very large x and y scales and two components with the same scale as the topography. Examination of the individual amplitudes shows that

$A_0 \sim 1/l_0$, so that $A_0 e^{i l_0 y}$ contributes a term in the perturbation streamfunction which is proportional to y —a modification of the zonal mean flow. This suggests an alternative approach, which is to consider the zonal x -averaged momentum equation and the equation for the deviations. We begin with the quasi-geostrophic equations for a homogeneous fluid,

$$f_0 v = p_x,$$

$$f_0 u = -p_y,$$

$$u_t + (uv)_x + (uv)_y - \beta y v - f_0 v^{(1)} = -p_x^{(1)},$$

$$v_t + (uv)_x + (v^2)_y + \beta y u + f_0 u^{(1)} = -p_y^{(1)},$$

$$u_x^{(1)} + v_y^{(1)} - \frac{1}{H} [(ub)_x + (vb)_y] = 0,$$

and consider the zonally averaged equations

$$\langle v \rangle = 0,$$

$$\langle u \rangle_t + \langle uv \rangle_y = f_0 \langle v^{(1)} \rangle,$$

$$\langle v^{(1)} \rangle_y = \frac{1}{H} \langle vb \rangle_y.$$

If the topography vanishes at some y far from the region of interest [following the arguments suggested by Hart (1979b), who showed that the Charney-DeVore truncated spectral problem was identical to that of forced flow over topography varying slowly with y], we can integrate the last equation to find

$$\langle u \rangle_t + \langle uv \rangle_y = \frac{f_0}{H} \langle vb \rangle.$$

The vorticity equation can be used to find the x -dependent part of the flow. In particular, if we assume the y scale is very large, we can drop all y derivatives to get two coupled equations:

$$\langle u \rangle_t = \frac{f_0}{H} \langle vb \rangle,$$

$$v_{xt} + \langle u \rangle v_{xx} + \beta v = -\frac{f_0}{H} \langle u \rangle b_x.$$

For the topography $b = b_0 \sin kx$, we have a steady solution

$$\langle u \rangle = \bar{u},$$

$$v = Ak \cos kx.$$

The deviations from this state satisfy

$$\langle u \rangle'_t = \frac{1}{2} \frac{f_0 b_0}{H} \langle v' \sin kx \rangle,$$

$$v'_{xt} + \bar{u} v'_{xx} + \beta v' = k \left(Ak^2 - \frac{f_0 b_0}{H} \right) \langle u \rangle' \cos kx$$

$$= k \frac{f_0 b_0}{H} \frac{\beta}{\bar{u} k^2 - \beta} \langle u \rangle' \cos kx,$$

which may be solved explicitly to give the dispersion relation (18.63). Here too one sees that it is the coupling between the change in the zonal flow induced by the wave drag and the change in the waves due to changes in zonal flow which leads to the instability. If we decrease the mean flow for a supercritical case (i.e., if we take $\langle u \rangle'$ to be negative), we produce low vorticity on the upwind slopes of the topography and high vorticity on the lee slopes. Associated with this vorticity change is high pressure on the upslope side of the mountains and low pressure on the downslope. This pressure pushes eastward on the topography so that the topography pushes westward on the fluid and decelerates the mean flow still further.

Flow in the Presence of Topography The previous section has described the influence of wavy topography upon the stability of the flows that go over it. However, there also exists topography that does not alter the mean-flow structure, either because the mean current is parallel to the topographic contours or because the currents occur only at levels above the peaks of the topography. In this section, we shall show that the stability of a parallel mean flow in the presence of topography can be quite different from that of the identical mean flow in a flat-bottomed ocean. We have been guided by the result of Charney and Straus (1980), who show that the form-drag instability can catalyze the release of available potential energy in a baroclinic shearing flow that would be stable in the absence of topography. In their study of multiple equilibria and stability in forced baroclinic flow over topography, they found that form-drag instability may occur for weaker thermal driving than conventional baroclinic instability, and that this type of instability leads to transition from one finite-amplitude, quasi-stationary equilibrium state to another. Baroclinic and barotropic instabilities of the stationary topographically perturbed flows give rise to westward-propagating, vacillating wave motions with periods of the order of 5 to 15 days. They suggest that the form-drag instability leads to transition from one stationary regime to another and that the observed westward- and eastward-propagating long planetary waves (zonal wavenumbers 1-4) are the propagating instabilities associated with these stationary regimes.

The simplest and most obvious example of the destabilizing effect of topography is the case of zonal barotropic flow with meridionally varying topography. The topography alters the effective value of β and thereby the growth rates and stability criteria: even though the energy source remains the horizontal shear, the topography can alter the possibility of extracting this energy. In particular, the Charney-Stern necessary criterion for instability [that $\beta - \bar{u}_{yy} + (f_0/H) b_y$ must

change sign in the domain] suggests that instability may occur for lower values of shear when $b_y \neq 0$. The necessary condition may, of course, not be sufficient; in particular, when $\bar{u}_y = 0$, the flow will be stable even if $\beta + (f_0/H)b_y$ changes sign. However, in the case of sinusoidal $\bar{u}(y)$ and $b(y)$, the necessary condition seems also to be sufficient (using a simple truncated expansion in y), and the topography does destabilize the flow.

DeSzoeke (1975) discussed baroclinic flow over meridionally varying topography and found that the topography destabilizes the flow at some wavenumbers by a resonant instability involving two baroclinic waves which happen to travel at the same speed. Similar effects can be identified in the work of Durney (1977). We would like to focus our discussion, however, on the specific problem of destabilization by form-drag instability of a baroclinic flow which is neutrally stable in the absence of topography.

We shall consider the conventional two-layer model whose governing equations (cf. Pedlosky, 1979b) are

$$\begin{aligned} & \left(\frac{\partial}{\partial t} + \mathbf{v}_1 \cdot \nabla \right) \\ & \times \left[\nabla^2 \psi_1 - \frac{\lambda_1^2}{1 + \delta} (\psi_1 - \psi_2) + \beta y \right] = 0, \\ & \left(\frac{\partial}{\partial t} + \mathbf{v}_2 \cdot \nabla \right) \\ & \times \left[\nabla^2 \psi_2 - \frac{\delta \lambda_1^2}{1 + \delta} (\psi_2 - \psi_1) + \beta y + \frac{f_0}{H} (1 + \delta) b \right] = 0, \end{aligned}$$

where \mathbf{v}_1 and ψ_1 are the velocity and streamfunction in the upper layer and \mathbf{v}_2 and ψ_2 the corresponding quantities in the lower layer, δ is the ratio of the upper to the lower layer mean depths, and λ_1^{-1} is the layered version of the first baroclinic mode deformation radius $\lambda_1^2 = f_0 (1 + \delta)^2 / g(\Delta\rho/\rho)H\delta$. We write the x -averaged equations

$$\begin{aligned} & \frac{\partial}{\partial t} \left[-\bar{u}_{1yy} + \frac{\lambda^2}{1 + \delta} (\bar{u}_1 - \bar{u}_2) \right] \\ & + \frac{\partial^2}{\partial y^2} \overline{\psi'_{1x} \left(\frac{\partial^2}{\partial y^2} \psi'_1 + \frac{\lambda^2}{1 + \delta} \psi'_2 \right)} = 0, \\ & \frac{\partial}{\partial t} \left[-\bar{u}_{2yy} + \frac{\delta \lambda^2}{1 + \delta} (\bar{u}_2 - \bar{u}_1) \right] \\ & + \frac{\partial^2}{\partial y^2} \overline{\psi'_{2x} \left(\frac{\partial^2}{\partial y^2} \psi'_2 + \frac{\delta \lambda^2}{1 + \delta} \psi'_1 \right)} = -\frac{f_0}{H} (1 + \delta) \frac{\partial^2}{\partial y^2} \overline{\psi'_{2x} b}, \end{aligned}$$

and the equations for the deviations

$$\begin{aligned} & \left(\frac{\partial}{\partial t} + \bar{u}_1 \frac{\partial}{\partial x} \right) \left[\nabla^2 \psi'_1 - \frac{\lambda^2}{1 + \delta} (\psi'_1 - \psi'_2) \right] \\ & + \left[\beta + \frac{\lambda^2}{1 + \delta} (\bar{u}_1 - \bar{u}_2) \right] \psi'_{1x} \end{aligned}$$

$$\begin{aligned}
& + J \left[\psi'_1, \nabla^2 \psi'_1 - \frac{\lambda^2}{1 + \delta} (\psi'_2 - \psi'_1) \right] \\
& - \frac{\partial}{\partial y} \overline{\psi'_{1x} (\psi'_{1yy} + \frac{\lambda^2}{1 + \delta} \psi'_2)} = 0, \\
& \left(\frac{\partial}{\partial t} + \bar{u}_2 \frac{\partial}{\partial x} \right) \left[\nabla^2 \psi'_2 - \frac{\delta \lambda^2}{1 + \delta} (\psi'_2 - \psi'_1) \right. \\
& \left. + \frac{f_0}{H} (1 + \delta) b \right] + \left[\beta - \frac{\delta \lambda^2}{1 + \delta} (\bar{u}_1 - \bar{u}_2) \right] \psi'_{2x} \\
& + J \left[\psi'_2, \nabla^2 \psi'_2 - \frac{\delta \lambda^2}{1 + \delta} (\psi'_2 - \psi'_1) + \frac{f_0}{H} (1 + \delta) b \right] \\
& - \frac{\partial}{\partial y} \overline{\psi'_{2x} \left[\psi'_{2yy} + \frac{\delta \lambda^2}{1 + \delta} \psi'_1 + \frac{f_0}{H} (1 + \delta) b \right]} = 0.
\end{aligned}$$

If we now consider y scales that are order $1/\Delta$ of the x scales or the deformation scale and expand $\bar{u}_i = \bar{u}_i^{(0)} + \Delta^2 \bar{u}_i^{(1)} + \dots$, $\psi'_i(x, y) = \psi'_i^{(0)}(x) + \Delta^2 \psi'_i^{(1)}(x, y) + \dots$ (where the topography is assumed to vary only in x) we find

$$\bar{u}_i^{(0)} = \bar{u}_{2i}^{(0)},$$

so that the induced changes in mean flow are barotropic. This occurs because the form-drag forcing of the mean is at much larger scales than the deformation scale. Eliminating the $\bar{u}_i^{(1)}$ terms at second order from the two mean flow equations, noting that the Reynolds stresses drop out because $\psi'_i^{(0)}$ is independent of y , we find that the barotropic component of the zonal flow is accelerated or decelerated by the form drag,

$$\frac{\partial \bar{u}_2}{\partial t} = \frac{f_0}{H} \overline{\psi'_{2x} b}, \quad (18.64)$$

while the deviation fields are given by

$$\begin{aligned}
& \left[\frac{\partial}{\partial t} + (\bar{u}_2(t) + \Delta u) \frac{\partial}{\partial x} \right] \left[\psi'_{1xx} - \frac{\lambda^2}{1 + \delta} (\psi'_1 - \psi'_2) \right] \\
& + \left(\beta + \frac{\lambda^2 \Delta u}{1 + \delta} \right) \psi'_{1x} = 0, \quad (18.65)
\end{aligned}$$

$$\begin{aligned}
& \left[\frac{\partial}{\partial t} + \bar{u}_2 \frac{\partial}{\partial x} \right] \left[\psi'_{2xx} - \frac{\delta \lambda^2}{1 + \delta} (\psi'_2 - \psi'_1) \right] \\
& + \left(\beta - \frac{\delta \lambda^2 \Delta u}{1 + \delta} \right) \psi'_{2x} = -\frac{f_0}{H} (1 + \delta) \bar{u}_2 b_x. \quad (18.66)
\end{aligned}$$

Here we have dropped the superscript (0) and introduced the notation Δu for the *time-independent* shear across the interface.

From the equations (18.64)–(18.66) one could derive a single nonlinear governing equation for \bar{u}_2 and determine the linear instability and finite-amplitude evolution of the flow. For our purposes, however, it will be sufficient to demonstrate that the initial state $\bar{u}_2 = 0$, $\psi'_1 = 0$, $\psi'_2 = 0$ can be unstable in the presence

of weak topography to infinitesimal perturbations even when the flow would be baroclinically stable in the absence of topography. We can do this by considering the stability in the special case $\Delta u = \beta(1 + \delta)/\delta \lambda^2$. This is the maximum shear for which the Rayleigh necessary criterion for stability in the absence of topography,

$$\left(\beta - \frac{\delta \lambda^2}{1 + \delta} \Delta u \right) \left(\beta + \frac{\lambda^2}{1 + \delta} \Delta u \right) \geq 0,$$

is satisfied. Equations (18.14)–(18.16) simplify to the set

$$\begin{aligned}
& \frac{\partial \bar{u}_2}{\partial t} = \frac{f_0}{H} \overline{\psi'_{2x} b}, \\
& \left[\frac{\partial}{\partial t} + \frac{\beta(1 + \delta)}{\delta \lambda_1^2} \frac{\partial}{\partial x} \right] \left[\psi'_{1xx} - \frac{\lambda_1^2}{1 + \delta} (\psi'_1 - \psi'_2) \right] \\
& + \beta \left(\frac{1 + \delta}{\delta} \right) \psi'_{1x} = 0,
\end{aligned}$$

$$\frac{\partial}{\partial t} \left[\psi'_{2xx} - \frac{\delta \lambda_1^2}{1 + \delta} (\psi'_2 - \psi'_1) \right] = -\frac{f_0}{H} (1 + \delta) \bar{u}_2 b_x.$$

We split the streamfunction into sine and cosine parts as in section 18.7.3 and solve this system of equations to find the growth rate equation

$$\begin{aligned}
& \sigma^4 \left(\frac{\delta}{1 + \delta} \right)^2 k^2 (k^2 + \lambda^2)^2 \\
& + \sigma^2 \left[\frac{\beta^2}{\lambda^4} \left(k^4 - \frac{\delta}{1 + \delta} \lambda^4 \right)^2 \right. \\
& \left. + \frac{1}{2} \left(\frac{f_0 b_0}{H} \right)^2 \frac{\delta^2}{1 + \delta} k^2 \left(k^2 + \frac{\lambda^2}{1 + \delta} \right) (k^2 + \lambda^2) \right] \\
& + \frac{1 + \delta}{2} \frac{\beta^2}{\lambda^2} \left(\frac{f_0 b_0}{H} \right)^2 k^2 \left(k^2 - \frac{\delta}{1 + \delta} \lambda^2 \right) \left(k^4 - \frac{\delta}{1 + \delta} \lambda^4 \right) \\
& = 0. \quad (18.67)
\end{aligned}$$

The real solutions to (18.67) for several values of $f_0 b_0 \lambda / \beta H$ are shown in figure 18.16. Notice the instability occurring for topographic scales on the order of 70 to 110 km, with growth rates proportional to the topographic height (for small heights, at least). We have thus demonstrated that the available potential energy in the flow can be tapped by the orographic instability even in situations where normal baroclinic instability is unable to extract mean-flow energy. Thus it is possible that mesoscale topography plays a role in catalyzing the conversion of mean flow potential to eddy energy in the oceans.

18.7.4 Multiple Equilibria

We have already mentioned the work of Charney and DeVore (1979) and Charney and Straus (1980), who have begun to explore the possibility that the atmosphere may possess a multiplicity of steady equilibrium

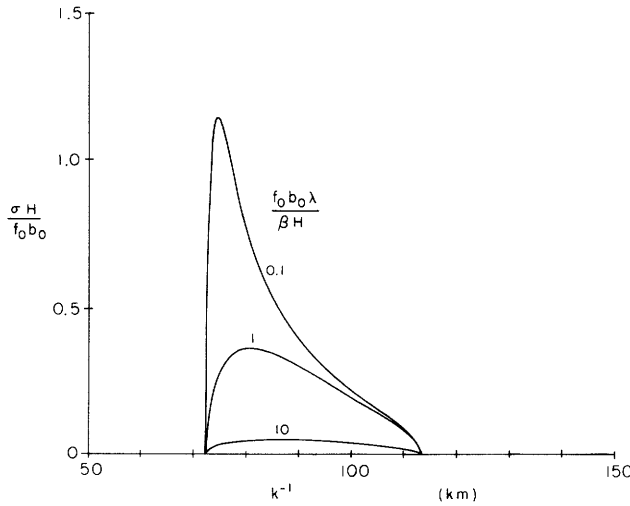


Figure 18.16 Normalized growth rates for a topographically destabilized vertical shear flow. The curves are labeled by $f_0 b_0 \lambda / \beta H$ values.

states for given external forcing in the presence of topographic inhomogeneities. In the case of sinusoidal topography in a periodic channel, they have found states resembling both the “normal” configuration in which there is a strong zonal flow and a relatively weak wave perturbation, and the “blocking” configuration in which there is a weak zonal flow and a relatively strong wave perturbation. They suggest that the blocking phenomenon is an equilibrium state which occurs by a transition via a form-drag instability from the normal to the anomalous blocking configuration. Hart (1979b) has applied similar ideas to laboratory flows and has succeeded in producing stationary multiple equilibria experimentally.

Oceanically, one phenomenon that stands out as a possible example of multiple quasi-stable equilibrium states is the large meander of the Kuroshio which sometimes occurs. Figure 18.17 shows the two quasi-stable configurations that are observed. The transitions between these configurations occur relatively rapidly. White and McCreary (1976) have considered a model for the meandering process involving flow around bumps in the Japanese coastline. Because their discussion was in terms of linear dynamics, Solomon (1978) has rightly pointed out that the model must have a smooth transition between the two states as the independent variable (the maximum inlet flow speed) varies. If, however, the phenomenon is nonlinear, catastrophic changes in the state of the Kuroshio may occur: an infinitely small change in parameters may produce a finite change in response, and several stable responses may be possible for the same set of parameters.

We propose a simple model of this process consisting of the steady, nonlinear flow of barotropic current on

a β -plane along a variable coastline (see figure 18.18). Let the latitude of the coastline be $h(x)$ and let η be the north-south distance from the coastline. The potential vorticity equation becomes

$$\left[\left(\frac{\partial}{\partial x} - h_x \frac{\partial}{\partial \eta} \right)^2 + \frac{\partial^2}{\partial \eta^2} \right] \psi + \beta(\eta + h) = F(\psi).$$

If we split the streamfunction into an upstream part ($x \rightarrow -\infty, h \rightarrow 0$) $\bar{\psi}(\eta)$ and a topographically induced part $\phi(x, \eta)$ we find

$$\left[\left(\frac{\partial}{\partial x} - h_x \frac{\partial}{\partial \eta} \right)^2 + \frac{\partial^2}{\partial \eta^2} \right] \phi = F(\bar{\psi} + \phi) - F(\bar{\psi}) - \beta h - \bar{\psi}_{\eta\eta} h_x^2, \quad (18.68)$$

where

$$F(\bar{\psi}(\eta)) = \beta \eta + \frac{\partial^2 \bar{\psi}}{\partial \eta^2}, \quad (18.69)$$

$$\phi \rightarrow 0 \quad \text{for } \eta = 0, \quad \eta \rightarrow -\infty.$$

When $\bar{u} = -\partial \bar{\psi} / \partial \eta$ is not constant, equation (18.69) implies that F is a nonlinear functional, so that (18.68) becomes essentially a forced nonlinear oscillator equation; it is well known that such equations may have multiple stable solutions. We note also a similarity between the equations here and the equations for flow of a barotropic fluid over topography. In the derivation below we assume that the coastline variations are small and occur on scales large compared to the cross-stream scale. We shall show that the nonlinearity plays an important role in determining the amplitude of the nonzonal flow component when the upstream flow is near the critical speed U_c . This speed is defined by the condition that long waves (x wavelength large compared to the width of the current) are stationary. Near critical speeds, the amplitude becomes large. The lowest-order dynamic equation only determines the cross-stream wave structure. The first-order equation shows a balance between advection by the mean flow, effects of the coastline variations, dispersion, and nonlinearity.

We shall work with the nondimensional forms of (18.68)–(18.69). Our scaling is guided by the versions

$$\begin{aligned} \left(\frac{\partial^2}{\partial x^2} + \frac{\partial^2}{\partial \eta^2} \right) \phi &= -\beta h + F'(\bar{\psi}) \phi \\ &= -\beta h - \frac{\beta - \bar{u}_{\eta\eta}}{\bar{u}} \phi \end{aligned} \quad (18.70)$$

obtained by linearizing in ϕ and h . We obtain $F'(\bar{\psi})$ by differentiating (18.69). If $h = h_0 \cos kx$, resonance occurs when

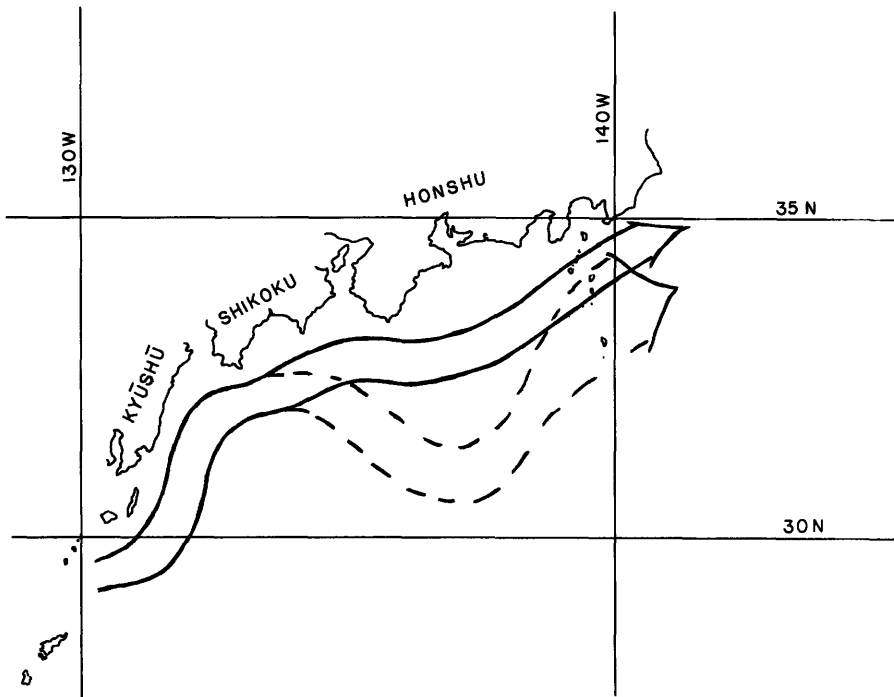


Figure 18.17 Sketch of two equilibrium positions of the Kuroshio. See Taft (1972) and White and McCreary (1976) for detailed tracks.

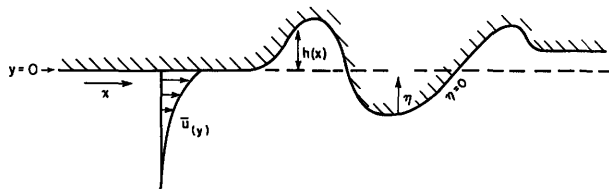


Figure 18.18 Model for coastline induced meandering. The deviation of the coastline from a latitude circle is denoted $h(x)$; the coordinate η is equal to $y - h(x)$. The upstream flow is $\bar{u}(y)$.

$$\left(\frac{\partial^2}{\partial \eta^2} + \frac{\beta - \bar{u}_{\eta\eta}}{\bar{u}} \right) \phi = k^2 \phi, \quad (18.71)$$

$$\phi = 0, \quad \eta = 0, -\infty.$$

For forcing on a scale long compared to the width of the current ($|\partial/\partial x| \ll |\partial/\partial \eta|$) we expect that one of the underlined terms in (18.70) will balance the forcing from the side-wall variations $-\beta h$ giving $\phi \sim U h_0$ or $\phi \sim \beta h_0 l^2$, where U is the scale of \bar{u} and l is the cross-stream scale. When the flow profile is nearly critical for long waves—meaning that the left-hand side of (18.71) vanishes for some nonzero function ϕ which also satisfies the boundary conditions, the long-wave solutions of (18.70) have the two underlined terms nearly canceling, so that the forcing must be balanced by the ϕ_{xx} term. This gives a scale of $\phi \sim \beta h_0 L^2$, where L is the downstream scale of variation of the topography.

Therefore, we scale x by L , h by h_0 , ϕ by $\beta h_0 L^2$, η by l , and \bar{u} by U in (18.68)–(18.69) to find

$$\left[\frac{\partial^2}{\partial \eta^2} + \delta \left(\frac{\partial}{\partial x} - \gamma \delta^2 h_x \frac{\partial}{\partial \eta} \right)^2 \right] \phi = -\delta h + \frac{1}{\gamma \delta} \left[F \left(\bar{\psi} + \frac{\gamma \delta}{M} \phi \right) - F(\bar{\psi}) \right] - \gamma M \delta^4 h_x^2 \bar{\psi}_{\eta\eta},$$

$$F(\bar{\psi}(\eta)) = \eta + M \bar{\psi}_{\eta\eta},$$

with $M = U/\beta l^2$, $\gamma = h_0 L^4/l^5$, and $\delta = l^2/L^2$. If we assume that the width of the current is small compared to the downstream scale ($\delta \ll 1$) and that the variations in coastline are weak enough so that $\gamma \lesssim 1$, we can simplify to

$$\left(\frac{\partial^2}{\partial \eta^2} + \delta \frac{\partial^2}{\partial x^2}\right) \phi = -\delta h + F'(\bar{\psi}) \frac{\phi}{M} + \frac{1}{2} F''(\bar{\psi}) \frac{\gamma \delta \phi^2}{M^2} + O(\delta^2) \quad (18.72)$$

$$\phi \rightarrow 0, \quad \eta = 0, -\infty,$$

with

$$F'(\bar{\psi}) = -\frac{1}{\bar{u}} (1 - M\bar{u}_{\eta\eta}), \quad (18.73)$$

$$F''(\bar{\psi}) = \frac{1}{\bar{u}} \frac{\partial}{\partial \eta} \left[\frac{1}{\bar{u}} (1 - M\bar{u}_{\eta\eta}) \right],$$

which are known functions of η given the specification of the upstream ($x \rightarrow -\infty$) flow $\bar{u}(\eta)$.

We assume that the flow is nearly critical so that $U = U_c(1 + \Delta)$ where U_c is the critical speed (defined exactly below) and therefore $M = M_c(1 + \Delta)$. We expand (18.72)-(18.73) assuming $\Delta \sim \delta$ and $M_c \sim 1$, $\gamma \leq 1$, and find to lowest order

$$\frac{\partial^2}{\partial \eta^2} \phi = \frac{\bar{u}_{\eta\eta} - M_c^{-1}}{\bar{u}} \phi, \quad (18.74)$$

$$\phi = 0, \quad \eta = 0, -\infty,$$

which defines the eigenvalue M_c and thus the critical speed U_c given the shape of the upstream flow. The η structure of ϕ must be an eigenfunction G of (18.74), $\phi = f(x)G(\eta)$. At next order in Δ and δ , the solvability condition for (18.72) gives

$$\left[\int_{-\infty}^0 d\eta G^2(\eta) \right] f''(x)$$

$$= -h(x) \left[\int_{-\infty}^0 d\eta G(\eta) \right] + \frac{\Delta}{\delta M_c} \left[\int_{-\infty}^0 G^2(\eta) / \bar{u}(\eta) \right] f(x)$$

$$+ \frac{1}{2} \left[\int_{-\infty}^0 d\eta G^3(\eta) \right] \frac{1}{\bar{u}} \frac{\partial}{\partial \eta} \left[\frac{1}{\bar{u}} (1 - M_c \bar{u}_{\eta\eta}) \right] \frac{\gamma}{M_c^2} f^2(x).$$

This ordinary differential equation for the x structure of the wave $f(x)$ is to be solved for a particular form as Δ/δ and γ vary. For convenience we shall normalize G and redefine parameters slightly to write

$$f'' - \hat{\Delta} f + \hat{\gamma} f^2 = -h(x). \quad (18.75)$$

The simplest problem to illustrate the characteristics of (18.75) is the linear case with $h(x) = \cos x$. (This topography extends to $x = -\infty$, which is not really consistent with our original model: however, it does point out some of the properties of these nonlinear flows.) The solution to (18.75) with $\hat{\gamma} = 0$ is

$$f = \frac{\cos x}{1 + \hat{\Delta}},$$

showing a resonance at $\hat{\Delta} = -1$ (see figure 18.19).

For weak nonlinearity ($\hat{\gamma}$ small), we can express f as a Fourier series

$$f = A \cos x + \hat{\gamma} (A_0 + A_2 \cos 2x) + \hat{\gamma}^2 \sum_{n=3}^{\infty} A_n \cos nx,$$

which implies a cubic equation for A :

$$(1 + \hat{\Delta})A - \hat{\Delta}^2 A^3 \left[\frac{1}{\hat{\Delta}} + \frac{1}{(4 + \hat{\Delta})} \right] = 1. \quad (18.76)$$

(One can show that the higher-order terms will not contribute, even near resonance.) Figure 18.19 also shows the solution of (18.76) for $\hat{\gamma} = 0.2$. Here we clearly see that there are three equilibrium states for $\hat{\Delta} < -1.3$. The state with intermediate amplitude is unstable; thus we see that we can have either a large positive amplitude wave (in phase with topography) or a small negative amplitude wave (out of phase).

This simple model suggests that the Kuroshio meander may be a case of multiple states depending on the flow rate at the inlet. Slight decreases in speed may cause a sudden transition to a meander state, with hysteresis effects likely, so that large increases are necessary before the Kuroshio would return to its path closer to the coast.

The above results merely suggest the possibility of multiple equilibria because, to begin with, we have required the coastline to have an infinite number of ridges and troughs in order to create the possibility of linear resonance. As shown in figure 18.10, an infinite number of periods may not be necessary, but there must be at least two ridges and a trough or vice versa. A single coastal ridge (as in the half-wave case) would not be enough to give a maximum response. One must

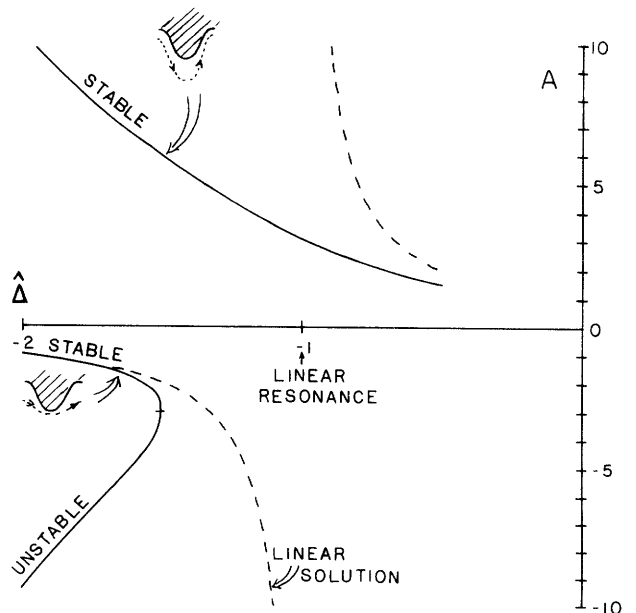


Figure 18.19 The wave amplitude as a function of $\hat{\Delta}$ (proportional to the magnitude of the upstream current). Sketches show the relationship between the streamlines and the coastline. Multiple equilibria occur for $\hat{\Delta} < -1.3$.

ask: Can a single ridge or, in the case of blocking in the atmosphere, a single mountain range, in an extended domain give rise to multiple equilibria? And is resonance needed?

In problems of nonrotating shallow-water flow over an obstacle, multiple states can exist when the Froude number \bar{u}/\sqrt{gH} is greater than unity. For certain values of the Froude number and the ratio of the obstacle height to H , two states are found, one corresponding to smooth flow with no upstream disturbance and one corresponding to a permanent elevation of the free surface upstream of the obstacle—created during the approach to equilibrium by a bore traveling upstream (Baines and Davies, 1980). Similar examples of multiple equilibria are also found in transonic compressible flow past obstacles. Thus we suspect that the upstream flow in our problem cannot be specified arbitrarily but may very well be affected by the upstream propagation of energy. It may be that, as in the periodic models of Charney-DeVore and Charney-Straus, the flow must be dealt with as a global or basin-wide unit.

18.7.5 Quasi-Geostrophic Turbulence

We have considered only wave-wave or wave-mean flow interactions involving a small number of components. In particular, we have not considered energy-cascade processes involving large numbers of components and leading ultimately to turbulent dissipation. It was pointed out by Onsager (1949), Lee (1951), Batchelor (1953a), and especially by Fjørtoft (1953) that vorticity conservation in two-dimensional flow imposes a strong constraint on scale interactions. Later Charney (1966, 1971a) showed that the conservation of pseudopotential vorticity in three-dimensional quasi-geostrophic flow imposes similar constraints. Such constraints suggested to Kraichnan (1967) that there may be an inertial subrange in two-dimensional, homogeneous, isotropic turbulence in which the energy spectrum is controlled by uniform transfer of enstrophy (mean-squared vorticity) from large to small scales at scales less than the excitation scale, and by uniform transfer of energy from small to large scales at scales greater than the excitation scale. He predicted a k^{-3} spectral energy density for scalar wavenumber k in the former range, and a Kolmogorov $k^{-5/3}$ law in the latter range. In extending these ideas to three-dimensional, quasigeostrophic turbulence, Charney (1971a) also obtained a k^{-3} law at the tail of the spectrum and conjectured that in this region there would also be equipartition between the two components of the kinetic energy and the available potential energy. This conjecture has been confirmed by Herring (1980) in a homogeneous quasi-geostrophic turbulence closure model.

The topic of quasi-geostrophic turbulence has been investigated by a number of oceanographers, notably Rhines (1975) by numerical simulation, and Holloway

and Hendershott (1977) and Salmon (1978) by means of closure [see also Herring (1980) and Leith (1971)]. It may be that their work is more applicable to the atmosphere than to ocean basins, where meridional boundaries play important roles and where statistical inhomogeneity of excitation cannot be ignored.

The existence of quadratic invariants, energy and enstrophy—mean-squared vorticity in two-dimensional or mean-squared pseudopotential vorticity in three-dimensional quasi-geostrophic flows—permits application of the principles of statistical mechanics. These have been applied by Onsager (1949) and Kraichnan (1975) to two-dimensional flow, and by Salmon, Holloway, and Hendershott (1976) to a two-layer quasi-geostrophic flow. In the two-dimensional case, the energy in each horizontal mode is $L^2/(b + aL^2)$, where a and b are constants depending on the total energy and enstrophy. With typical choices of these constants, the largest scale waves have the most energy. In the two-layer case, the equilibrium spectrum is dominated by the largest scales, and these motions are barotropic. The available potential-energy spectrum, corresponding to the thermocline displacement spectrum, is peaked near the deformation radius. These spectra represent the effects of the nonlinear terms alone; one expects [as Errico (1979) found in studying the partition of energy between gravity-wave and geostrophic motions] that the spectra which are actually realized in a forced and dissipative system will be determined largely by the wavenumber dependence of the forcing and dissipation.

The cornerstone for the theory of quasi-geostrophic turbulence is the conservation (in the inviscid limit) of the energy $\frac{1}{2} \iint |\nabla\psi|^2 + (1/S) \|\partial\psi/\partial z\|^2$ and the enstrophy $\frac{1}{2} \iint [(\nabla^2\psi + (\partial/\partial z)(1/S)(\partial\psi/\partial z))]^2$. We emphasize the fragility of the last principle: enstrophy can increase or decrease if there are (1) temperature gradients along horizontal boundaries, (2) side walls on the domain, or (3) topography.

If we first consider the case when none of these restrictions obtain—flow in a periodic, flat-bottomed domain—we can readily argue that the energy will be transferred to large horizontal scales and to more barotropic motions by the nonlinear terms. If we expand the streamfunction in the flat-bottomed normal modes and perform a Fourier transform horizontally,

$$\psi = \sum_n F_n(z) \iint d\mathbf{k} \hat{\psi}_n(\mathbf{k}, t) e^{i\mathbf{k}\cdot\mathbf{x}},$$

we can use the conservation principles

$$\frac{\partial}{\partial t} \sum_n \iint d\mathbf{k} (\mathbf{k}^2 + \lambda_n^2) |\hat{\psi}_n|^2 = 0,$$

$$\frac{\partial}{\partial t} \sum_n \iint d\mathbf{k} (\mathbf{k} + \lambda_n^2) |\hat{\psi}_n|^2 = 0$$

(λ_n is the reciprocal radius of deformation for the n th baroclinic mode; see section 18.5.1) in exactly the same manner as Fjørtoft (1953) or Charney (1971a) to show that the amount of energy with $k^2 + \lambda_n^2 > K_0^2$ is a small fraction of the initial energy, if K_0 is large compared to the initial mean wavenumber

$$\bar{K} = \frac{\sum_n \iint d\mathbf{k} (k^2 + \lambda_n^2)^{1/2} [(k^2 + \lambda_n^2)|\hat{\psi}|^2]}{\sum_n \iint d\mathbf{k} [(k^2 + \lambda_n^2)|\hat{\psi}|^2]}.$$

In essence the nonlinearity does not transfer energy to small scales. Another way to show the reverse cascade, is to use Rhines's (1975) argument that the turbulence spreads energy out in wavenumber space

$$\frac{\partial}{\partial t} \sum_n \iint d\mathbf{k} [(k^2 + \lambda_n^2)^{1/2} - \bar{K}]^2 [(k^2 + \lambda_n^2)|\hat{\psi}_n|^2] > 0.$$

Combining this with the definition of \bar{K} and using the conservation laws shows that the mean total wavenumber must decrease

$$\frac{\partial}{\partial t} \bar{K} < 0.$$

Thus energy cascades to larger horizontal *and* vertical scales, implying an increase in energy for small λ_n^2 , that is, a tendency for the motion to become more barotropic.

This tendency for the flow to become barotropic in the absence of topography or side walls has been well demonstrated through numerical simulation by Rhines (1977). He has also shown that rough topography can halt this cascade for flows that are not too energetic. The β -effect slows the cascade when the scale has increased so much that the wave steepness M becomes order one. This could occur while the motions are still baroclinic if the initial energy were small compared to $\beta^2 L_R^4$.

Rhines (1975) has also argued that side walls can stop the reverse cascade. This has been demonstrated in laboratory experiments by Colin de Verdière (1977). Essentially the western boundary serves as a source of enstrophy and the eastern boundary a sink. This can be understood—as Pedlosky (1967), in a slightly different context, has revealed—by considering reflection of Rossby waves from the western boundary. For linear waves with $c = -\beta/(k^2 + l^2 + \lambda_n^2)$, the x component of the group velocity is negative for $k^2 < (l^2 + \lambda_n^2)$. Therefore the reflected wave's zonal wavenumber $k_r = (l^2 + \lambda_n^2)/k$ is larger than k . One can readily show that the energy fluxes of the incident and reflected waves (c_g times the energy density) are equal and opposite, but that the enstrophy flux of the outgoing wave is larger by a factor k_r/k than the flux of the incident wave.

Rhines (1977) has discussed many of the topics above, and in particular has demonstrated clearly that

the strong nonlinear interactions involved in geostrophic turbulence cannot occur unless nonlinearity is much stronger than wave dispersion, that is, unless the wave steepness $Uk^2/\beta \gg 1$. At these scales there is some, but not conclusive, evidence in support of a k^{-3} spectrum for the atmosphere (Julian and Clive, 1974). The enstrophy cascade mechanism has not yet been checked adequately either by direct measurement or by numerical simulation. It remains possible that the observed atmospheric spectra can be explained in terms of ordered (periodic) frontal structures, rather than random cascades of enstrophy, as suggested by Andrews and Hoskins (1978). They obtain a $k^{-8/3}$ dependency which is as much in accord with observations as the k^{-3} spectrum—or perhaps better. However, the predicted spectra are highly anisotropic, and this does not seem to be in as good agreement with observations or results from numerical modeling as the predictions of the theory of geostrophic turbulence.

So far the data do not exist for a corresponding oceanic check.

18.8 Summary Remarks

Our primary focus has been on oceanic analogues of transient atmospheric motions of large scale. As promised in the introduction, it has been possible to find formal oceanic analogues for most categories of large-scale atmospheric motions: indeed, it has been almost trivial to do so. Far more difficult, however, has been to demonstrate the physical reality and importance of these analogues. It is only recently, through studies of the meanders of the western boundary currents and through such concentrated, large-scale observational programs as MODE, Polygon, POLYMODE, and the oceanographic component of the GARP Atlantic Tropical Experiment (GATE), that some understanding of the nature of the transient motions has begun to emerge. Although many of the oceanic analogues we have dealt with are hypothetical to a greater or lesser degree, we have chosen them on physical grounds as at least of potential importance. We feel that contrasting them with their atmospheric counterparts, with respect to both their individual properties and their roles in the generation and maintenance of the large-scale circulation patterns, has been a useful exercise.

In section 18.4, it is shown that the quasi-geostrophic, β -plane formalism derived for the atmosphere applies to oceanic motions whose horizontal scales are on the order of the deformation radius of the first baroclinic mode L_R , that is, the scales corresponding to baroclinic instability. It is characteristic of these motions that they are dispersive at both small and large amplitudes. At larger scales the dynamics change: linear free modes may no longer have the same east-west and north-south scales and vertical density advection

becomes an important cause of nonlinearity. For motions with length scales near the "intermediate scale" $(L_R^2 a)^{1/3}$ with velocities of order $f_0 L_R^2/a$ (where a is the radius of the earth), the vertical component of vorticity changes not only because of β -effects and horizontal advection but also because of vertical density advection and variation of the undifferentiated Coriolis parameter. Thus both Rossby and Burger terms appear. For east-west scales on the order of the intermediate scale (210 km for the ocean and 1500 km for the atmosphere) or larger, dispersion and nonlinearity can balance to give solitary or cnoidal waves. For larger scales, we show that the evolution is determined by a Korteweg-deVries equation, so that solitons will be the natural end product of the evolution of an initially isolated disturbance. Because of the slower dissipation and the larger scale separation between the intermediate and basin scales, such waves are more likely to be found in the ocean than in the atmosphere. These results suggest that the larger-scale dynamics of the ocean transients may be dominated by more orderly, phase-coherent structures than are predicted by the theory of geostrophic turbulence. If this is so, then at scales larger than the excitation scale the low-wavenumber components would be more highly correlated than if they were due to a random reverse cascade.

The theory of free and forced small-amplitude Rossby waves in the oceans may be transposed almost entirely from the corresponding atmospheric theory. The MODE and Polygon experiments have provided evidence of the importance of Rossby-wave propagation, particularly on time scales greater than a month (McWilliams, 1976). In section 18.5, we present some of this theory in an oceanographic context, paying particular attention to the influence of bottom topography in altering the propagation of free waves and in generating waves from a mean flow. Rhines's results for a uniformly stratified fluid are extended to arbitrarily stratified flows. The major result, the prediction of bottom-trapped modes, has been verified from observations at site D (Thompson, 1977) although no observations of the eastward-traveling modes which should exist when the topography opposes the β -effect have been reported.

The idea of Rossby-wave propagation in a medium with a variable (real or imaginary) index of refraction was first advanced to account for the vertical trapping of shorter waves by upper easterlies and strong westerlies. We apply these ideas in an oceanographic context not only to vertical propagation from the surface or bottom but also to horizontal propagation of waves generated by the meandering of the Gulf Stream. Eastward-propagating meanders produce trapped disturbances close to the Gulf Stream, while westward-propagating meanders may give a real index of refraction and southward propagation.

In section 18.6, we describe briefly the influence of friction both on the generation of ocean currents by wind and on the decay of individual oceanic eddies. Existing theory is not adequate to account for the spin-up of the real ocean or for the decay of the real atmospheric circulation. Interest in the baroclinic spin-down problem was originally motivated by a desire to understand the long persistence of Gulf Stream rings; however, the axisymmetric models that had previously been employed do not account for the complete decay of a baroclinic eddy. We show that the β -effect permits vertical propagation of energy and therefore allows for complete spin-down.

In the last section, we consider oceanic disturbances in which advective effects are important—either through wave-mean flow interaction as in the breakdown of an unstable mean flow, through the interaction of waves generated elsewhere with the local mean flow, or through wave-wave interactions. The last type of interaction can occur when the unstable flow is itself a wave or when waves generated in any manner interact with one another as in turbulence.

The concept of baroclinic instability was developed to explain the principal traveling waves and vortices embedded in the atmospheric westerlies; it has been applied to the oceans in an effort to account for the meandering of the western boundary currents and the existence of mid-ocean mesoscale eddies. The meandering does seem to be an effect of baroclinic instability, modified by barotropic effects, but it is highly questionable on theoretical and numerical-modeling grounds whether the mid-ocean eddies are due to local baroclinic instabilities. It seems more likely that these eddies are vortices cast off from, or forced in some more general fashion by, the meandering western boundary currents and their extensions.

In our exposition of the baroclinic and barotropic instability problem, we use the methods of Arnol'd and Blumen to extend the integral theorems of Kuo, Charney-Stern, and others to a class of basic flows that need not be zonal, that may translate with constant speed, and that may be influenced by topography.

The work on wave-mean flow interactions originated by Eliassen and Palm and Charney and Drazin in an atmospheric context is applied to the problem of the rectification of Rossby waves radiated from the western boundary currents and their extensions. Of particular interest is the so-called recirculation flow found by Worthington and others south of the Gulf Stream extension. Rhines has attempted to account for this recirculation as driven by the westward-propagating Rossby waves produced by the meandering. We present a slight generalization of his work by considering also the effects of eastward-traveling meanders. The results do suggest that a relatively strong westward flow, confined fairly close to the Gulf Stream, can be produced

by eastward-propagating wave-mean flow interactions in the presence of dissipation.

In recent times, the stability analyses for the atmosphere have been extended to wavy motions in an attempt to account for nonlinear cascades of energy in large-scale motions. The stability of forced wavy motions has also been studied to account for the transition from one stationary state to another of a forced flow over topography. It has been found from a study of simple truncated spectral models that the stationary flow equilibria produced by the forcing of a zonal flow over topography in a rotating system may be indeterminate in the sense that for a given forcing, there exists a multiplicity of equilibrium states. This result has been utilized in an attempt to explain the so-called blocking phenomenon in the atmosphere—the persistence of large-amplitude anticyclonic flow anomalies in the planetary circulation. The existence of multiple equilibria for a given forcing appears to be common; it also occurs for supercritical-Froude-number flow in hydraulics and transonic flow in gas dynamics. A natural oceanic analogue of multiple, quasi-stationary equilibrium in the atmosphere is the known existence of two states of flow for the Kuroshio in the vicinity of the Japanese coast. We investigate a simple model of such a flow and find indeed that two different steady states may be produced by a given upstream flow as it passes a wavy boundary. Our model leaves much to be desired, but it does point a direction for future research.

We find that the transition between one state and another in topographically forced flows occurs via a form-drag instability in which the perturbed form drag (mountain torque) modifies the mean flow in such a way that the perturbation increases in amplitude. The instability of a forced topographic wave is thus different from that of a free wave. The latter instability was shown by Gill to be basically a Rayleigh-like shear instability or a resonant-triad wave interaction. We have presented the wave-stability analysis for both free and forced waves in a unified fashion to bring out the similarities and differences between the shear, resonant, and form-drag instabilities.

The form-drag instabilities producing transition grow in place; however, the wavy equilibrium states themselves may also exhibit traveling Rayleigh-like instabilities. It has been suggested that instabilities of this kind account for the observed eastward- and westward-propagating very long (zonal wavenumbers 1–4) planetary waves in the atmosphere. One may speculate that a careful analysis of the topographically induced meanders of the western boundary currents in the ocean will also reveal such secondary wave instabilities. If these are westward propagating, then they could contribute to a broader recirculation region.

The final topic is quasi-geostrophic turbulence. Fjørtoft's prediction that there will be a transfer of energy

from the excitation scale to larger scales in 2-dimensional energy-and-entrophy-conserving flow may be extended to 3-dimensional quasi-geostrophic flows if the bottom and top boundaries are flat and isentropic. The theory predicts that the scale will increase vertically as well as horizontally, that is, that the flow will become increasingly barotropic at large horizontal scales. Rhines has verified this result in a series of numerical experiments, and the oceanic observations of Schmitz (1978) show that the mesoscale eddies tend to be more barotropic the more energetic they are. This observation, while not verifying the inertial theory of geostrophic turbulence, is at least consistent with it. As Rhines has shown, the inertial theory applies only when the effects of nonlinearity dominate those of linear dispersion, that is, when the wave steepness Uk^2/β is much greater than unity. Thus one expects the prediction to be valid only in the energetic parts of the ocean. The similarity prediction of a k^{-3} spectrum at scales smaller than the excitation scale is not inconsistent with observations in the atmosphere, but there are as yet no data to test this theory in the ocean. The effects of topography, side boundaries, and surface gradients of entropy also have not been thoroughly explored.

We have not produced a systematic or comprehensive treatment of atmosphere-ocean analogues. Our excuse, as we have stated, is that virtually all large-scale atmospheric motions have oceanic counterparts and there are simply too many of these to discuss. We have preferred to deal with analogues for which there is observational evidence or at least some physical basis for believing they should exist. We have been forced to speculate, and, as the reader will surely have perceived, our own speculations have been guided primarily by our own experience and interests.

Appendix: The Quasi-Geostrophic Equations

Here we shall give details of the derivations of the quasi-geostrophic equations. We begin by nondimensionalizing the equations of motion (18.22)–(18.27), using the definitions of the geostrophic streamfunction and the potential buoyancy b_p in (18.28) and (18.29). Using the characteristic scales described in the text, we obtain

$$\begin{aligned} \varepsilon \frac{Du}{Dt} + \omega \varepsilon \lambda \hat{\beta} \frac{uw \tan \Theta}{r} - \varepsilon \hat{\beta} \frac{uv \tan^2 \Theta}{r} - \lambda \omega \cot \Theta w - v \\ = -\frac{\alpha}{r} \frac{1}{\cos \Theta} \left(\frac{\partial}{\partial \phi} + \hat{\beta} \tan \Theta \frac{\partial}{\partial \Phi} \right) \psi, \end{aligned} \quad (18.A1)$$

$$\begin{aligned} \varepsilon \frac{Dv}{Dt} + \omega \varepsilon \lambda \hat{\beta} \frac{vw \tan \Theta}{r} + \varepsilon \hat{\beta} \frac{u^2 \tan^2 \Theta}{r} + u \\ = -\frac{\alpha}{r} \frac{1}{\sin \Theta} \left(\frac{\partial}{\partial \theta} + \hat{\beta} \tan \Theta \frac{\partial}{\partial \Theta} \right) \sin \Theta \psi, \end{aligned} \quad (18.A2)$$

$$\begin{aligned} & \omega\lambda^2\varepsilon\frac{Dw}{Dt} - \epsilon\lambda\hat{\beta}\tan\Theta\frac{u^2+v^2}{r} - \lambda u\cot\Theta \\ &= -\psi_z + \Delta\hat{S}\psi + b_p \\ & \quad - \epsilon\Delta(b_p - \Delta_s\psi)(\psi_z - \Delta\hat{S}\psi), \end{aligned} \quad (18.A3)$$

$$\begin{aligned} & \frac{1}{r\cos\Theta}\left(\frac{\partial}{\partial\phi} + \hat{\beta}\tan\Theta\frac{\partial}{\partial\Phi}\right)u + \frac{1}{r}\left(\frac{\partial}{\partial\theta} + \hat{\beta}\tan\Theta\frac{\partial}{\partial\Theta}\right)v \\ & - \frac{\hat{\beta}v\tan^2\Theta}{r} + \frac{\omega}{r^2}\frac{\partial}{\partial z}r^2w \\ &= \frac{\varepsilon\Delta}{\alpha}\frac{1}{\sin\Theta}\frac{D}{Dt}\sin\Theta(b_p - \Delta_s\psi) + \omega(\Delta_s + \Delta\hat{S})w \end{aligned} \quad (18.A4)$$

$$\begin{aligned} & \frac{1}{\alpha\sin\Theta}\frac{D}{Dt}\sin\Theta b_p + \frac{\omega}{\varepsilon}\hat{S}w + \frac{\omega\Delta_s}{\varepsilon\Delta}\left(1 - \frac{\alpha^2}{\hat{c}_s^2}\right)w \\ & - w\psi\frac{\omega\varepsilon}{\varepsilon}\frac{\partial}{\partial z}\Delta_s + \omega\frac{\varepsilon}{\varepsilon}(\Delta\hat{S} \\ & + \Delta_s)\left[b_p - \Delta_s\left(1 + \frac{\alpha^2}{\hat{c}_s^2}\right)\psi\right]w \\ & + \left(\frac{\alpha^2}{\hat{c}_s^2} - 1\right)\Delta_s\frac{1}{\sin\Theta}\frac{D}{Dt}\sin\Theta\psi = 0, \end{aligned} \quad (18.A5)$$

where

$$\begin{aligned} \frac{D}{Dt} &= \frac{\partial}{\partial t} + \frac{\varepsilon}{r}\left[\frac{u}{\cos\Theta}\left(\frac{\partial}{\partial\phi} + \hat{\beta}\tan\Theta\frac{\partial}{\partial\Phi}\right) \right. \\ & \quad \left. + \frac{v}{r}\left(\frac{\partial}{\partial\theta} + \hat{\beta}\tan\Theta\frac{\partial}{\partial\Theta}\right) + \omega w\frac{\partial}{\partial z}\right] \end{aligned}$$

and

$$\begin{aligned} r &= 1 + \lambda\hat{\beta}\tan\Theta z, \\ \alpha &= 1 + \epsilon\Delta(b_p - \Delta_s\psi), \\ \hat{c}_s^2 &= c_s^2/\bar{c}_s^2 = 1 + O(\epsilon\Delta) \end{aligned}$$

are used as abbreviations.

The quasi-Boussinesq approximation entails choosing the scale of motion to be small compared to the external radius of deformation $\Delta \ll 1$. We therefore drop terms from (18.A1)–(18.A5) which are small in this sense. The definition of “small” requires some care because the various Rossby numbers are also small. Thus in equations (18.A1), (18.A2), (18.A4) we shall keep both order 1 and order ε , ϵ , $\hat{\beta}$, ω terms so that we may drop only terms of order $\epsilon\Delta$, $\varepsilon\Delta$, $\omega\Delta$. Equations (18.A1) and (18.A2) are changed only slightly: α is replaced by 1. The other equations become

$$\begin{aligned} & \frac{1}{r\cos\Theta}\left(\frac{\partial}{\partial\phi} + \hat{\beta}\tan\Theta\frac{\partial}{\partial\Phi}\right)u + \frac{1}{r}\left(\frac{\partial}{\partial\theta} + \hat{\beta}\tan\Theta\frac{\partial}{\partial\Theta}\right)v \\ & - \frac{\hat{\beta}v\tan^2\Theta}{r} + \frac{\omega}{r^2}\frac{\partial}{\partial z}r^2w = \Delta_s\omega w, \end{aligned} \quad (18.A6)$$

$$\begin{aligned} & \omega\lambda^2\varepsilon\frac{Dw}{Dt} - \epsilon\lambda\hat{\beta}\tan\Theta\frac{u^2+v^2}{r} - \lambda u\cot\Theta \\ &= -\psi_z + b_p, \end{aligned} \quad (18.A7)$$

$$\begin{aligned} & \frac{1}{\sin\Theta}\frac{D}{Dt}\sin\Theta b_p + \frac{\omega}{\varepsilon}\hat{S}w - \omega\frac{\varepsilon}{\varepsilon}w\psi\frac{\partial}{\partial z}\Delta_s \\ & + \frac{\omega}{\varepsilon}\Delta_s\epsilon\left(\frac{\hat{c}_s^2-1}{\epsilon\Delta}\right)w - \frac{\omega\epsilon}{\varepsilon}\Delta_s(b_p - \Delta_s\psi)w = 0. \end{aligned} \quad (18.A8)$$

For the ocean, we can further refine these equations by noting that Δ_s is also very small, so that the continuity equation (18.A6) becomes that of an incompressible fluid, and the potential buoyancy equation becomes simply

$$\frac{1}{\sin\Theta}\frac{D}{Dt}\sin\Theta b_p + \frac{\omega}{\varepsilon}\hat{S}w = 0. \quad (18.A9)$$

The hydrostatic approximation applies to a thin layer of fluid: $\lambda \ll 1$. This allows us to drop the centrifugal terms involving w , the vertical accelerations, and to replace r by 1, giving us

$$\begin{aligned} & \varepsilon\frac{Du}{Dt} - \epsilon\hat{\beta}uv\tan^2\Theta - v \\ &= -\frac{1}{\cos\Theta}\left(\frac{\partial}{\partial\phi} + \hat{\beta}\tan\Theta\frac{\partial}{\partial\Phi}\right)\psi, \end{aligned} \quad (18.A10)$$

$$\begin{aligned} & \varepsilon\frac{Dv}{Dt} + \epsilon\hat{\beta}u^2\tan^2\Theta + u \\ &= -\frac{1}{\sin\Theta}\left(\frac{\partial}{\partial\theta} + \hat{\beta}\tan\Theta\frac{\partial}{\partial\Theta}\right)\sin\Theta\psi, \end{aligned} \quad (18.A11)$$

$$\begin{aligned} & \frac{1}{\cos\Theta}\left(\frac{\partial}{\partial\phi} + \hat{\beta}\tan\Theta\frac{\partial}{\partial\Phi}\right)u + \left(\frac{\partial}{\partial\theta} + \hat{\beta}\tan\Theta\frac{\partial}{\partial\Theta}\right)v \\ & - \hat{\beta}v\tan^2\Theta + \omega\frac{\partial w}{\partial z} = 0, \end{aligned} \quad (18.A12)$$

$$\psi_z = b_p, \quad (18.A13)$$

$$\begin{aligned} & \frac{1}{\cos\Theta}\left(\frac{\partial}{\partial\phi} + \hat{\beta}\tan\Theta\frac{\partial}{\partial\Phi}\right)u + \left(\frac{\partial}{\partial\theta} + \hat{\beta}\tan\Theta\frac{\partial}{\partial\Theta}\right)v \\ & - \hat{\beta}v\tan\Theta + \omega\frac{\partial w}{\partial z} = 0, \end{aligned} \quad (18.A14)$$

where

$$\begin{aligned} \frac{D}{Dt} &= \frac{\partial}{\partial t} + \frac{\varepsilon}{\varepsilon}\frac{u}{\cos\Theta}\left(\frac{\partial}{\partial\phi} + \hat{\beta}\tan\Theta\frac{\partial}{\partial\Phi}\right) \\ & \quad + \frac{\varepsilon}{\varepsilon}v\left(\frac{\partial}{\partial\theta} + \hat{\beta}\tan\Theta\frac{\partial}{\partial\Theta}\right) + \omega w\frac{\partial}{\partial z}. \end{aligned}$$

Equations (18.A9)–(18.A14) are the Boussinesq hydrostatic equations.

Finally, the quasi-geostrophic β -plane approximation assumes that $\hat{\beta} \sim \varepsilon \sim \epsilon \ll 1$ and (by necessity) that ω

must also be of this order. We set $\omega = \varepsilon$ and expand in powers of ε to find the lowest-order balances

$$u^{(0)} = -\frac{\partial\psi^{(0)}}{\partial\theta},$$

$$v^{(0)} = \frac{1}{\cos\Theta} \frac{\partial\psi^{(0)}}{\partial\phi},$$

$$b_p^{(0)} = \frac{\partial\psi^{(0)}}{\partial z}$$

and the continuity equation

$$\frac{1}{\cos\Theta} \frac{\partial u^{(0)}}{\partial\phi} + \frac{\partial v^{(0)}}{\partial\theta} = 0$$

which is consistent with the geostrophic equations. At first order we have the momentum equations

$$\varepsilon \frac{\hat{D}u^{(0)}}{Dt} - \varepsilon v^{(1)} = -\frac{1}{\cos\Theta} \frac{\partial}{\partial\phi} \varepsilon\psi^{(1)} - \frac{\hat{\beta} \tan\Theta}{\cos\Theta} \frac{\partial}{\partial\Phi} \psi^{(0)},$$

$$\varepsilon \frac{\hat{D}v^{(0)}}{Dt} + \varepsilon u^{(1)} = -\frac{1}{\sin\Theta} \frac{\partial}{\partial\theta} \varepsilon \sin\Theta \psi^{(1)} - \frac{\hat{\beta}}{\cos\Theta} \frac{\partial}{\partial\theta} \sin\Theta \psi^{(0)},$$

$$\frac{\hat{D}}{Dt} = \frac{\partial}{\partial t} + \frac{\varepsilon}{\cos\Theta} \frac{u^{(0)}}{\partial\phi} + \frac{\varepsilon}{\sin\Theta} \frac{v^{(0)}}{\partial\theta},$$

from which we form the vorticity equation

$$\begin{aligned} \varepsilon \frac{\hat{D}}{Dt} \left(\frac{v_{\phi}^{(0)}}{\cos\Theta} - u_{\theta}^{(0)} \right) + \varepsilon \left(\frac{u_{\phi}^{(1)}}{\cos\Theta} + v_{\theta}^{(1)} \right) \\ = -\hat{\beta} \frac{1}{\cos^2\Theta} \frac{\partial}{\partial\theta} \sin\Theta \frac{\partial\psi^{(0)}}{\partial\phi} + \hat{\beta} \frac{\sin\Theta}{\cos^2\Theta} \frac{\partial}{\partial\Phi} \frac{\partial\psi^{(0)}}{\partial\theta} \\ = -\hat{\beta} v^{(0)} - \hat{\beta} \frac{\sin\Theta}{\cos\Theta} \frac{\partial v^{(0)}}{\partial\theta} + \hat{\beta} \tan^2\Theta v^{(0)} - \hat{\beta} \frac{\sin\Theta}{\cos^2\Theta} \frac{\partial u^{(0)}}{\partial\Phi}. \end{aligned}$$

Combining this with the first-order continuity equation

$$\begin{aligned} \frac{\varepsilon}{\cos\Theta} u_{\phi}^{(1)} + \varepsilon v_{\theta}^{(1)} + \hat{\beta} \frac{\sin\Theta}{\cos^2\Theta} u_{\phi}^{(0)} + \hat{\beta} \tan\Theta \frac{\partial v^{(0)}}{\partial\theta} \\ - \hat{\beta} v^{(0)} \tan^2\Theta + \varepsilon \frac{\partial w^{(0)}}{\partial z} = 0 \end{aligned}$$

(note that for the atmosphere, we would have an additional term $-\Delta_s \varepsilon w^{(0)}$ in this equation) leads to the vorticity equation

$$\frac{\hat{D}}{Dt} \left(\frac{v_{\phi}^{(0)}}{\cos\Theta} - u_{\theta}^{(0)} \right) + \frac{\hat{\beta}}{\varepsilon} v^{(0)} = w_z^{(0)}.$$

The lowest-order potential-buoyancy equation

$$\frac{\hat{D}}{Dt} \psi_z^{(0)} + \hat{S} w^{(0)} = 0$$

can now be combined with the vorticity equation to give the quasigeostrophic conservation equation:

$$\begin{aligned} \frac{\hat{D}}{Dt} \left[\frac{1}{\cos\Theta} \frac{\partial}{\partial\phi} \frac{1}{\cos\Theta} \frac{\partial}{\partial\phi} \psi^{(0)} + \frac{\partial^2}{\partial\theta^2} \psi^{(0)} + \frac{\partial}{\partial z} \frac{1}{\hat{S}} \frac{\partial}{\partial z} \psi^{(0)} \right] \\ + \frac{\hat{\beta}}{\varepsilon} \frac{\psi_{\phi}^{(0)}}{\cos\Theta} = 0. \end{aligned}$$

For the atmosphere, the additional term in the continuity equation appears as an extra contribution

$$-\frac{\Delta_s}{\hat{S}} \frac{\partial}{\partial z} \psi^{(0)}$$

in the potential vorticity. Alternatively, the thickness term can be written as

$$\frac{\partial}{\partial z} \frac{1}{\alpha \hat{S}(z)} \frac{\partial}{\partial z} \psi$$

for atmospheric quasi-geostrophic motions.

Notes

1. Unfortunately, meteorologists use "mesoscale" very differently from oceanographers. We shall use mesoscale in the oceanic sense to refer to motions that are dynamically analogous to the "synoptic" scale motions of the atmosphere.
2. Note that the U here is characteristic of the disturbances, not of the mean flow.
3. Some care needs to be used in the cnoidal wave case since the mean depth of the fluid becomes $H + (1/2\pi L) \int_0^{2\pi} dx \eta$ and the last term does not vanish. For the figures we have corrected for this effect to show c nondimensionalized by βL_R^2 where L_R is based on the actual average depth. Thus we have plotted $c_{\text{actual}} = (1 - \varepsilon \langle \eta \rangle / \hat{S}_{\text{actual}}) c$ as a function of $\hat{S}_{\text{actual}} = \hat{S} + \varepsilon \langle \eta \rangle$, and also subtracted out the mean from the plots of $\phi^{(0)}$. The same process was used for the nonlinear Rossby wave but had no effect on the dispersion relation.
4. The "anelastic equations" (Batchelor, 1953b; Ogura and Charney, 1962; Ogura and Phillips, 1962) filter only acoustic waves.
5. It is customary to call any quasi-geostrophic wave a Rossby wave.
6. Geisler and Dickinson (1975) studied critical layer absorption in the western boundary current but did not explicitly include a reflected wave. It is also possible that the effects of the mechanisms maintaining the western boundary current are important in the interaction process.
7. It can be shown trivially that there is no nonlinear interaction in a spectrum of Rossby waves with all components having the same scale $[k^2 + \lambda^2]^{-1/2}$ (including baroclinic effects).